CMS HGCAL

A High Granularity Calorimeter for High Luminosity LHC

Shubham Pandey, IISER Pune

Argonne National Lab seminar
28 July 2021

Large Hadron Collider (LHC)

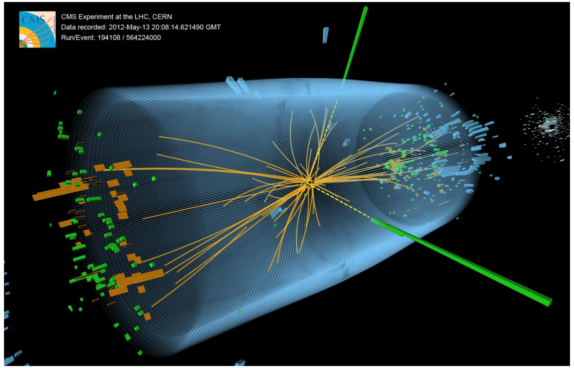

p-p collision @ √s = 13 TeV

Detect the outcome of collision

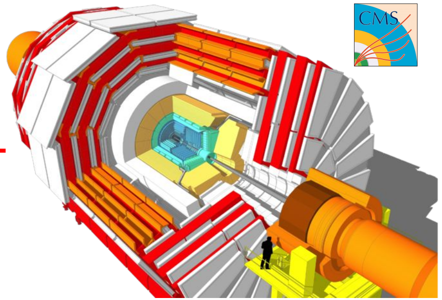

Compact Muon Solenoid (CMS)

Superconducting solenoid
- 3.8 T magnetic field

Iron return yoke
- Return path for magnetic field

Muons
- Drift Tubes (DT)
- Resistive plate chambers (RPCs)

HCAL
- Scint. interleaved b/w brass
- Energy measurement of charged & neutral hadrons

ECAL
- $PbWO_4$ crystals
- Energy measurement of **e**/γ

Tracker
- Si based pixels & strip
- Tracks charged particles

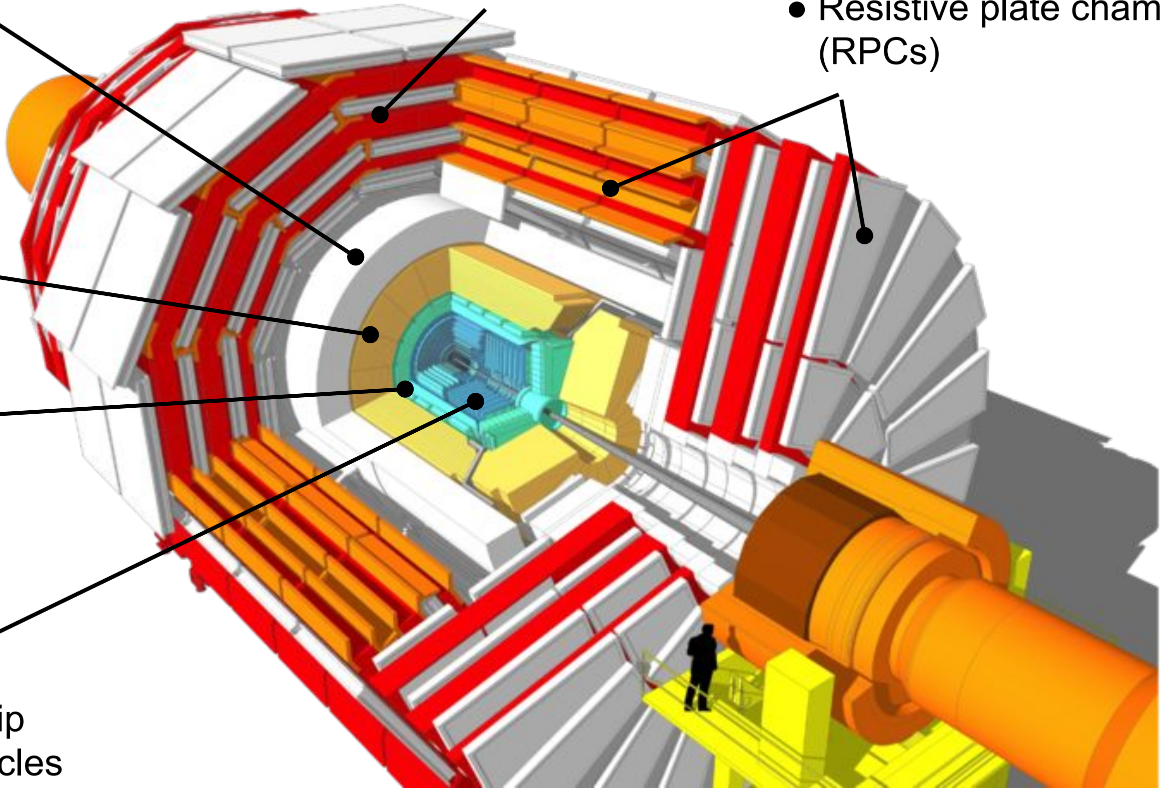

Particle reconstruction in CMS

Objects/events are reconstructed by combining information from different sub-detectors.

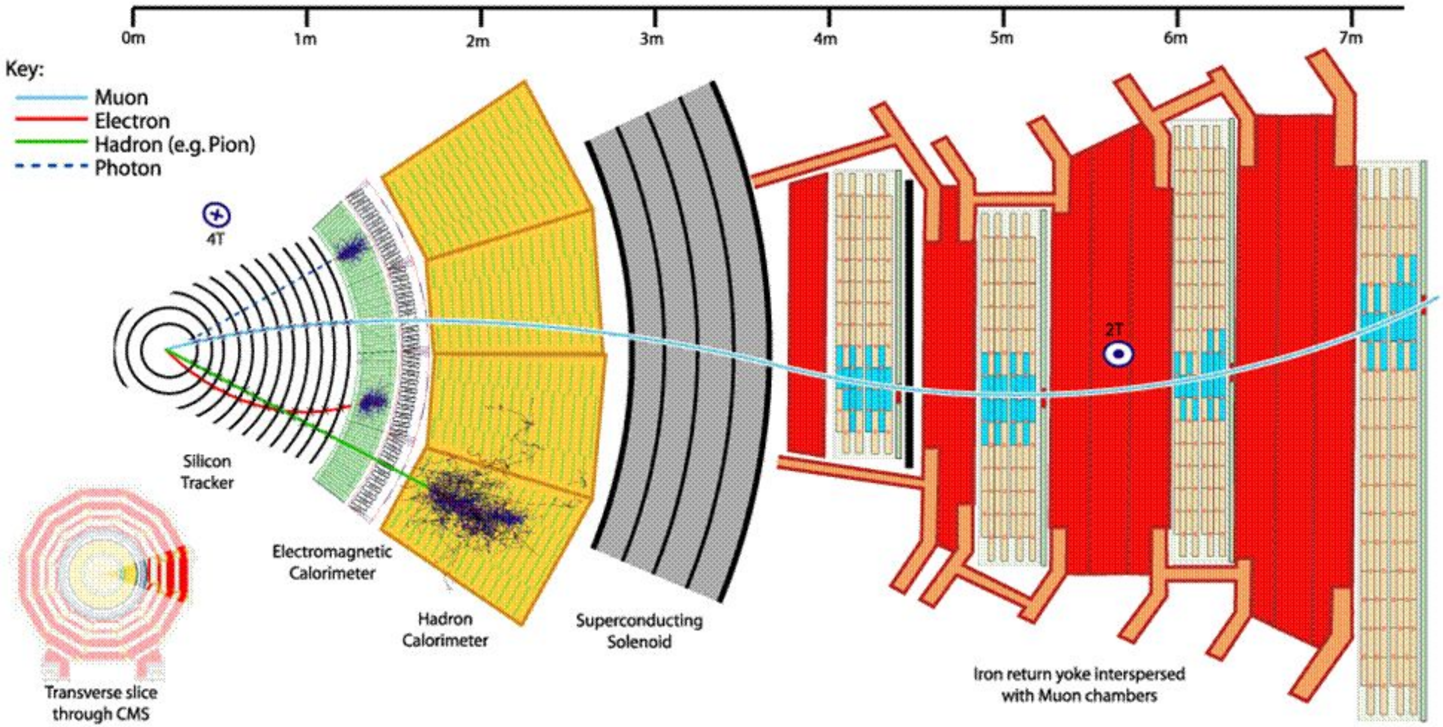

Concept is called “**Particle Flow**”.

The Luminosity plans & High Luminosity-LHC

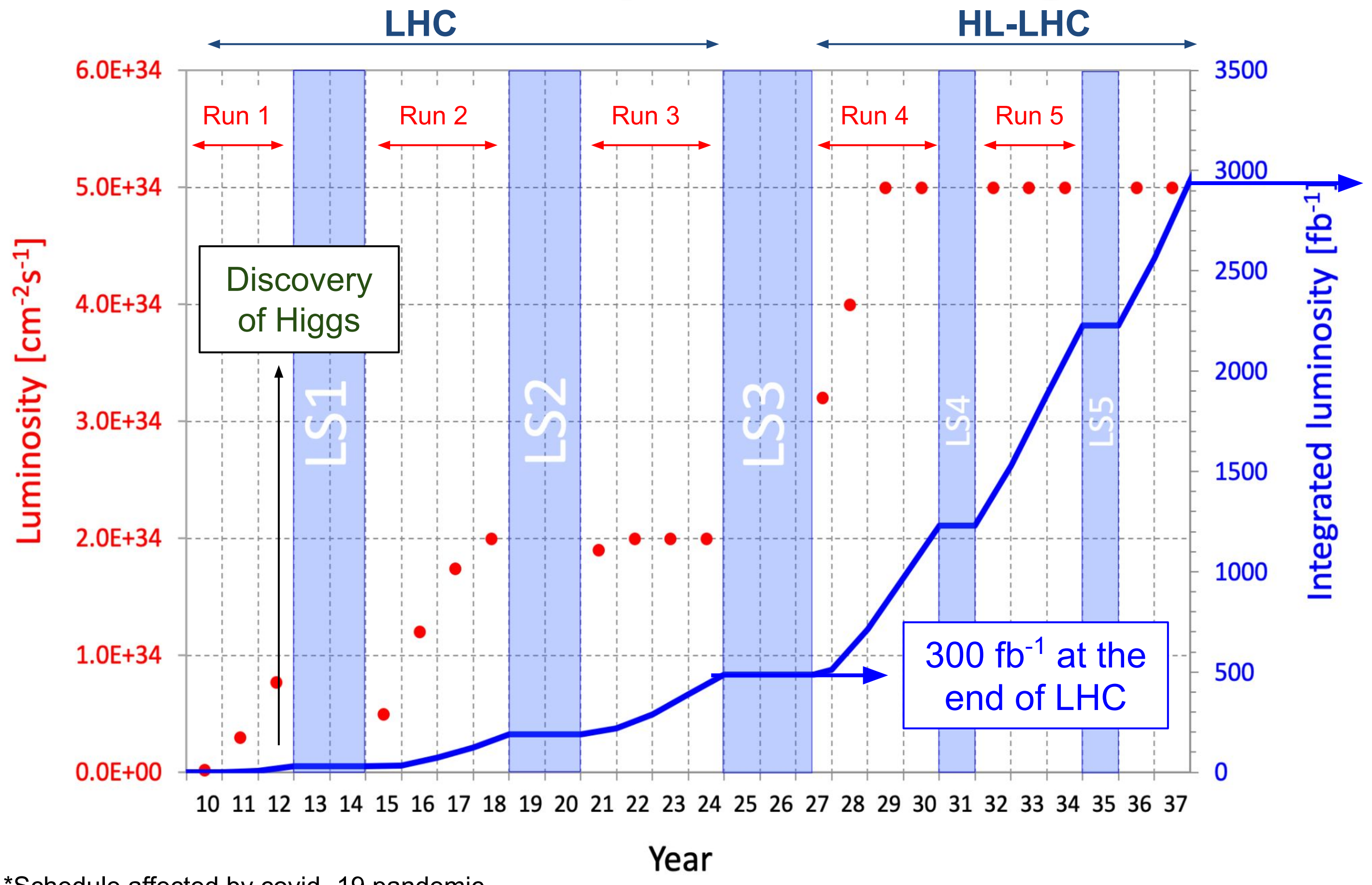

$3000\ fb^{-1}$ at the end of HL-LHC

-10x more int. lumi.

-Precision measurement to test the limit of SM

-Direct searches for new physics

Challenges for detectors !!

*Schedule affected by covid -19 pandemic

Challenges for CMS @HL-LHC: Radiation damage

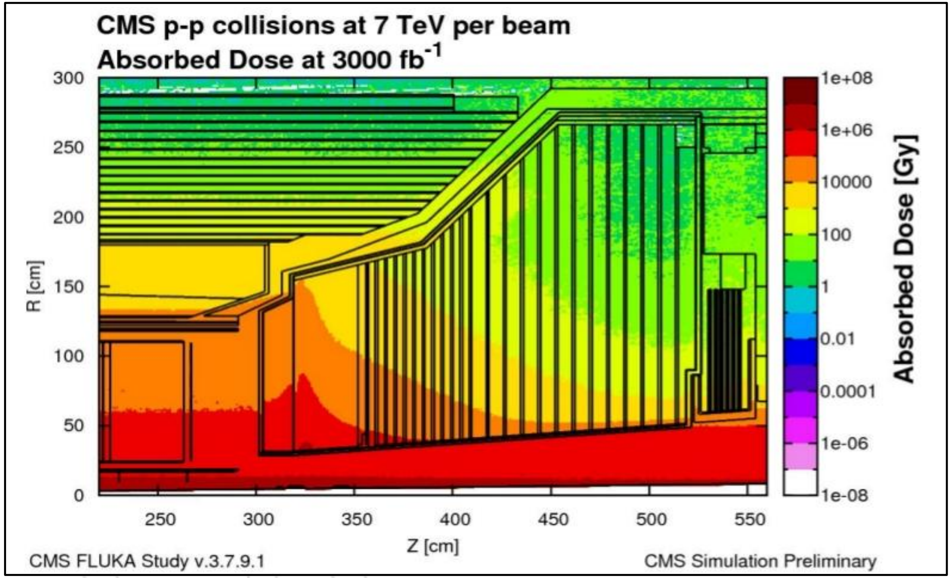

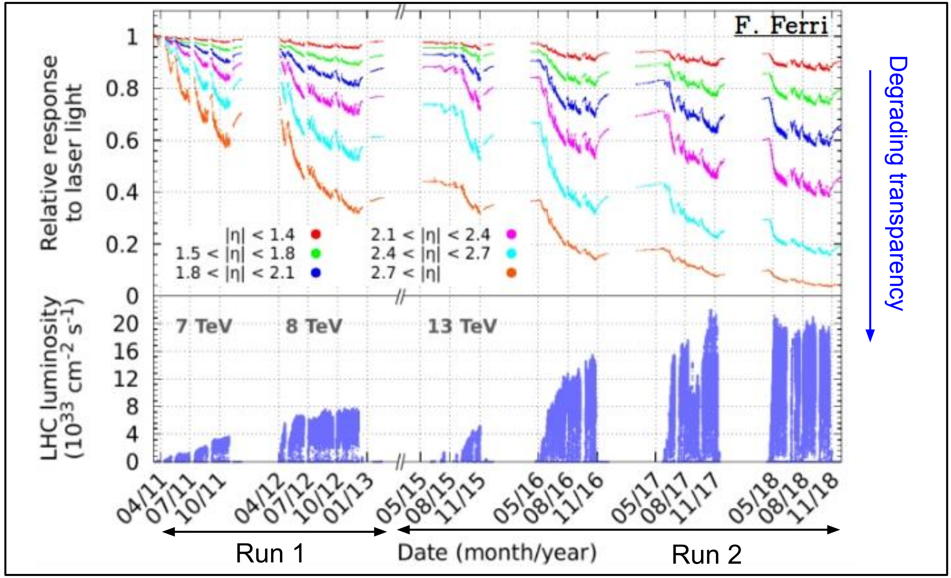

- ➢ Very high radiation dose in the detector.
- ➢ More radiation damage in the forward region.

- ➢ ECAL crystals are already losing transparency.
- ➢ Physics performance beyond acceptance by the end of Run3.

More radiation tolerant detector in the forward region is required !!

Challenges for CMS @HL-LHC: Pileup

➢ Very high pileup at the collision points.
  - Pileup: secondary p-p interactions
  - Contributes to increased complexity for tracking and adds extra energy for objects, e.g. jets.

➢ Average pileup will increase from **~37- 40** in Run 2 to ~**140 - 200** at HL-LHC.

➢ Extremely harsh environment for the detectors.

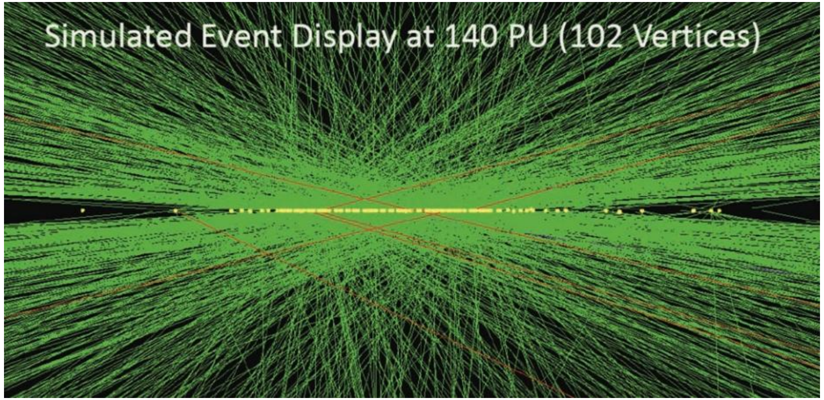

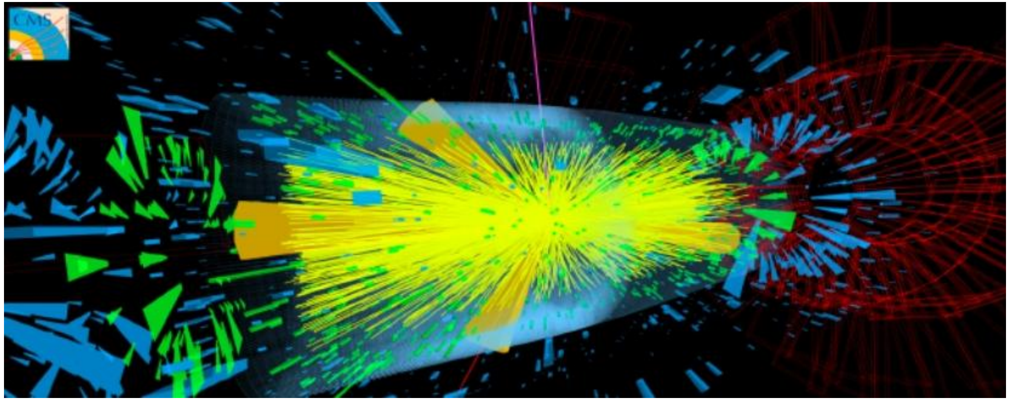

Pileup mitigation: More granular detector for shower separation & good timing capability for vertex/track association.

CMS upgrade for HL-LHC

Muons
- GEM/RPC in endcaps
- New DT FE electronics

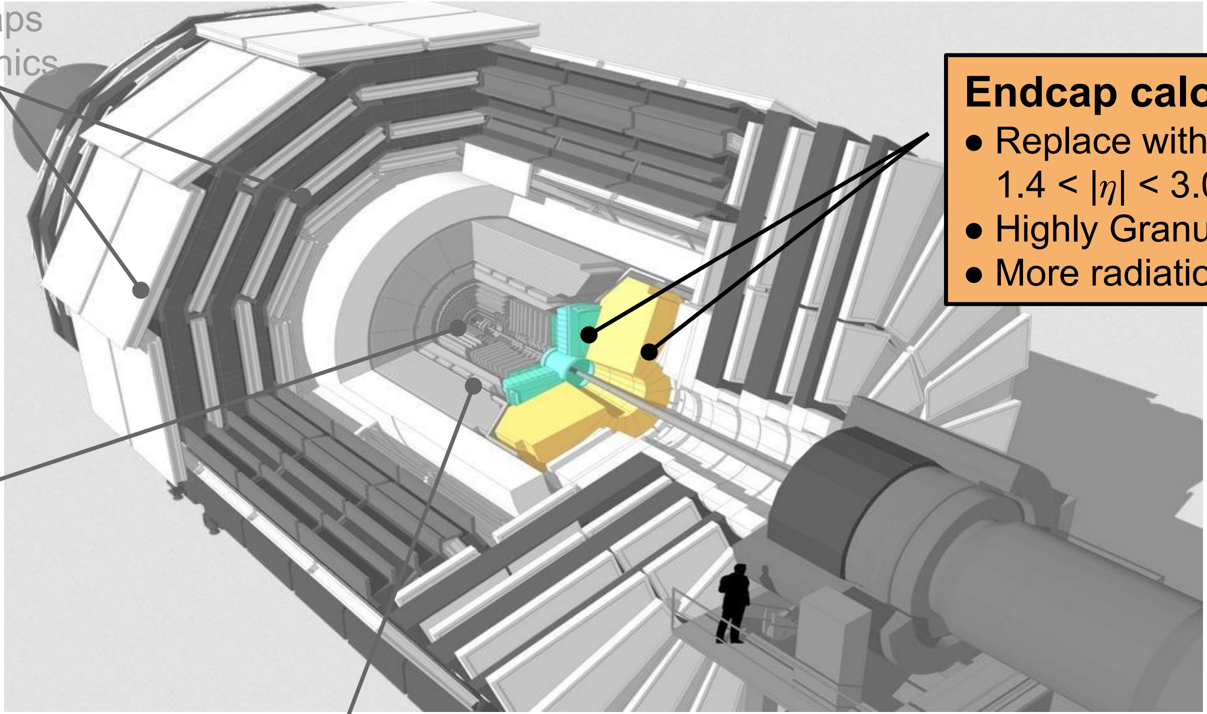

Endcap calorimeter
- Replace with new detector $1.4 < |\eta| < 3.0$
- Highly Granular
- More radiation tolerant

New Tracker
- More granular
- Less material
- $\eta \sim 4$

Triggers
- Level 1 (H/W) ~ 500 kHz to 1 MHz
- Tracks at L1
- HLT ~ 10 kHz

ECAL barrel
- Replace FE electronics

High Granularity CALorimeter

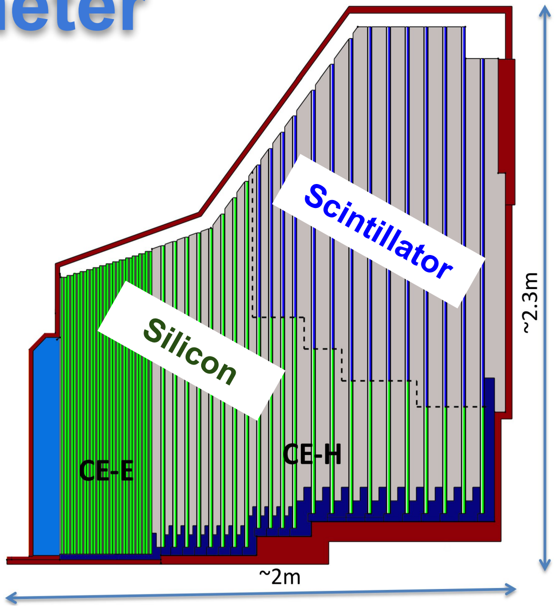

Active Elements:

- 8” hexagonal shaped **silicon** sensor modules in high radiation region in electromagnetic (CE-E) and hadronic section (CE-H).
- **Scintillator** tiles mounted on SiPM in the low radiation region in hadronic section.

HGCAL: Sampling Calorimeter

- **Electromagnetic part: CE-E**
  - **Si** sensors as active layers, Cu/CuW/Pb absorber
  - **28 layers, 25 X_0** and **~ 1.3 λ_{int}**
- **Hadronic part: CE-H**
  - **Si** & **scintillator** as active layers, steel absorbers
  - **22 layers, ~ 8.5 λ_{int}**

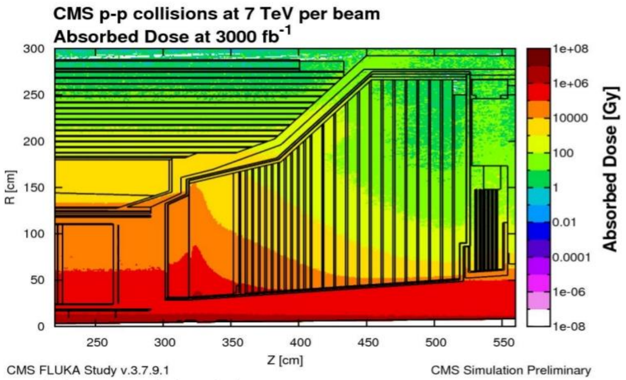

HGCAL: Features

Key-parameters:

- HGCAL coverage 1.5 < |η| < 3.0
- Full system maintained at -30°C
- Cell sizes: ~0.5 - 1.1 cm^2
- **~600 m^2** of Si sensors & **~500 m^2** of scintillators
- **6M Si & 240k Scint. readout channels**
- ~50 ps timing measurement

➔ Radiation tolerance ✔
➔ Dense : preserves shower compactness ✔
➔ Fine longitudinal & lateral granularity: shower separation ✔
➔ Good timing capability ✔

Efficient particle-flow reconstruction

Effective pileup mitigation

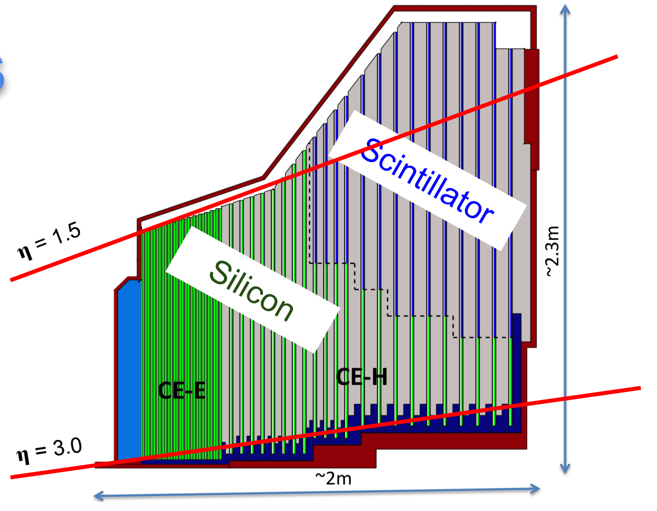

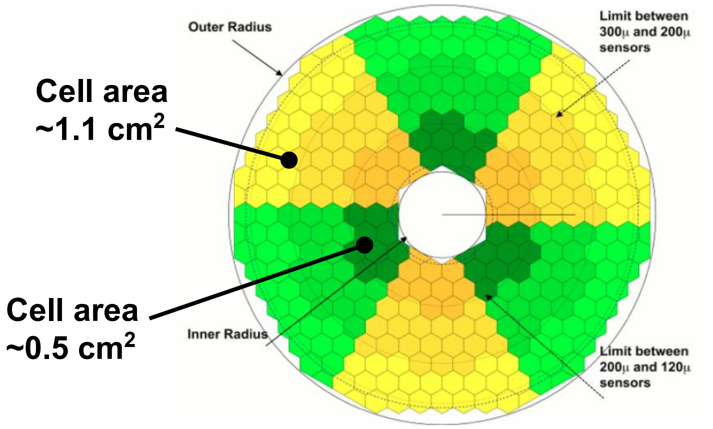

One disk in CE-E

HGCAL: from conceptualization to realization

Concept:

- ➔ Requirement
- ➔ Detector design
- ➔ Electrical & mechanics
- ➔ Performance studies based on Monte-Carlo

Prototype:

- ➔ Sensor & detector prototypes
- ➔ Performance studies based on real data
- ➔ Design improvement in multiple iterations

Installation:

- ➔ Manufacturing and assembly
- ➔ Full scale detector
- ➔ Installation

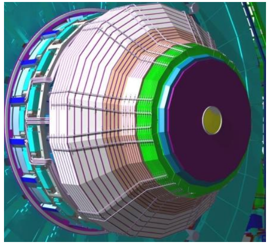

Technical design report

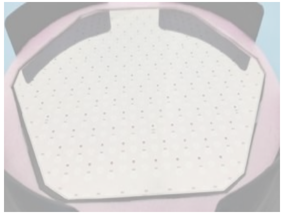

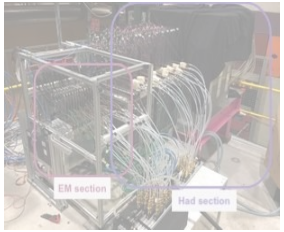

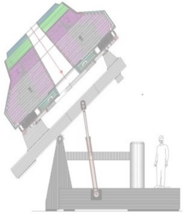

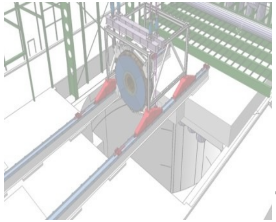

HGCAL: from conceptualization to realization

Concept:

- ➔ Requirement
- ➔ Detector design
- ➔ Electrical & mechanics
- ➔ Performance studies based on Monte-Carlo

Prototype:

- ➔ Sensor & detector prototypes
- ➔ Performance studies based on real data
- ➔ Design improvement in multiple iterations

Installation:

- ➔ Manufacturing and assembly
- ➔ Full scale detector
- ➔ Installation

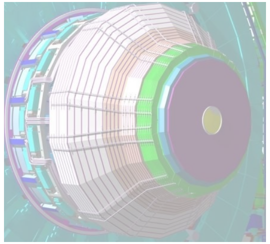

Technical design report

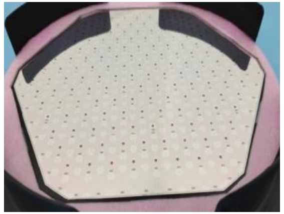

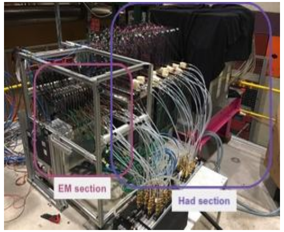

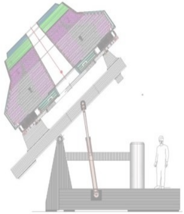

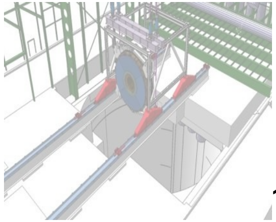

6" Silicon sensor prototype v2016

Gold plated layer

- To provide contact for bias voltage

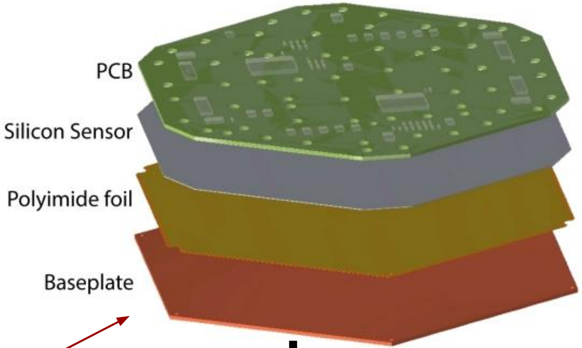

Glue together

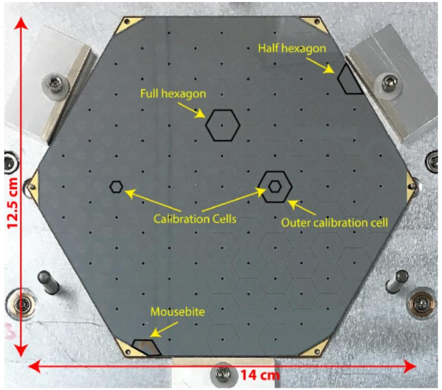

6" silicon sensor module

128 silicon cells
- p-on-n type Si
- 200 or 300 μm active thickness
- Area ~ 1.1 cm^2

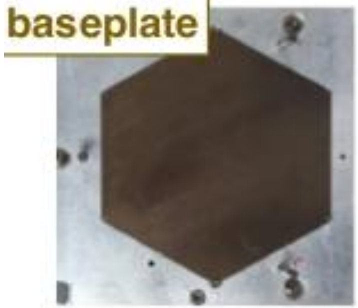

Cu/CuW or PCB

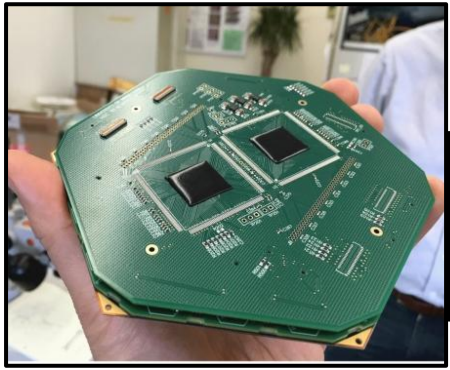

→ **First prototype module**
→ **SkiROC2 ASIC : 64 channel per chip readout**
→ **Two ASICs per module**
→ **Double PCB design**

System tests of silicon sensor module

➔ Each module has to undergo quality assurance test.
- ◆ Prototype is rejected if failed in test.

➔ Performed such a system test for silicon sensor prototypes (v2016) at CERN:
- ◆ IV characterisation ✓
- ◆ Connection and communication with data acquisition (DAQ) system ✓
- ◆ Pedestal/noise level measurement ✓
- ◆ Measured energy deposited by cosmic muons in si cells. ✓

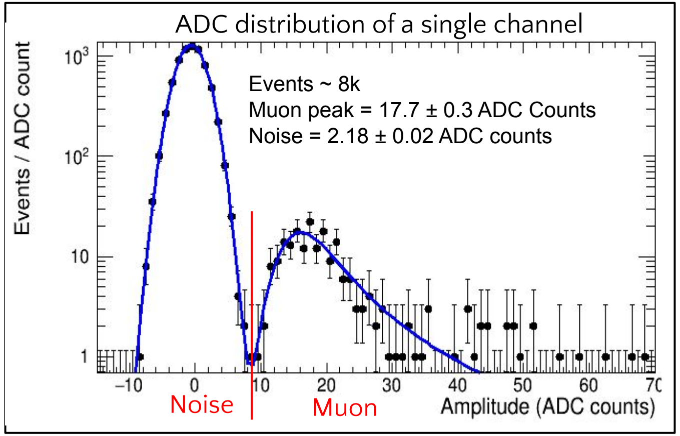

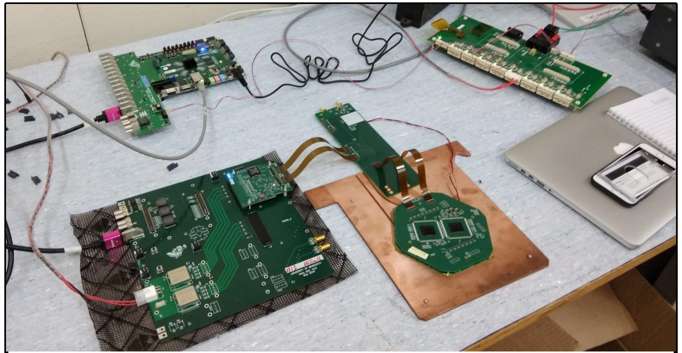

Si sensor module connected to DAQ chain

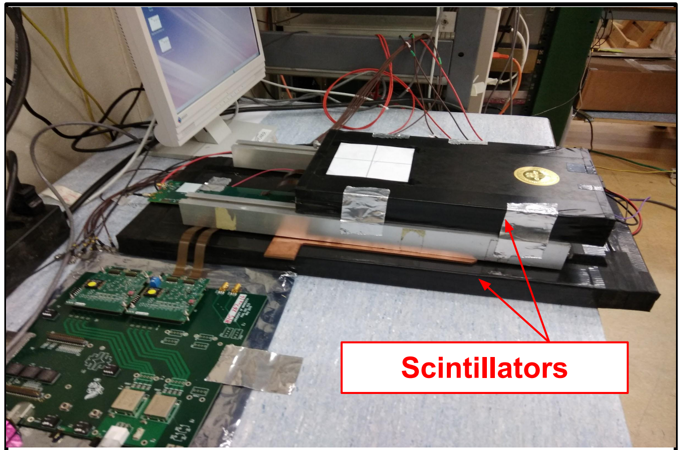

cosmic stand: Si module sandwiched between scint.

Updated 6” sensor module prototype

New module prototype version:

- Double PCB → single PCB design with added electronics
  - More compact form
- Updated ASIC: **SkiROC2-CMS**
  - Timing measurement: Time-Over-Threshold (ToT) & Time-of-Arrival (ToA)
- Four ASICs per module
  - Minimizes path lengths
- Two types of silicon sensor active thicknesses
  - 200 μm and 300 μm

Detailed system tests for v2018 module have been carried out.

v2016

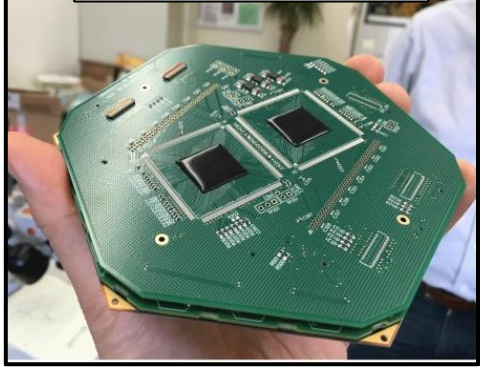

v2018

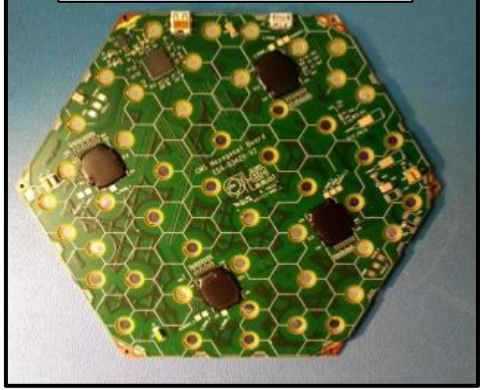

From sensor prototype to detector prototype

- ➢ Having tested the sensor prototype in lab based test benches → build a detector prototype.
- ➢ A prototype of electromagnetic (EM) and hadronic (Had) section of HGCAL was built with silicon sensor modules (v2018),
  - ○ Tested with the beams of single particles at CERN during October 2018.
- ➢ Evaluate the performance of the detector prototype.

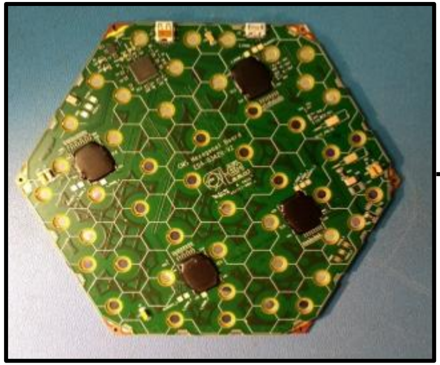

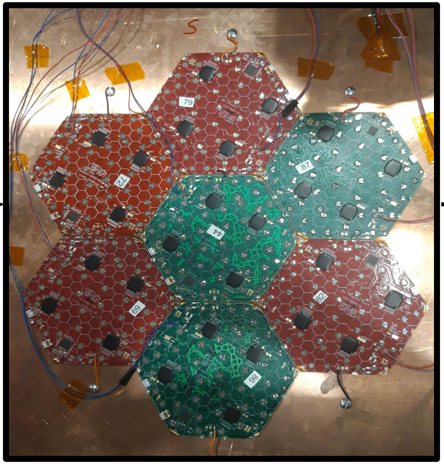

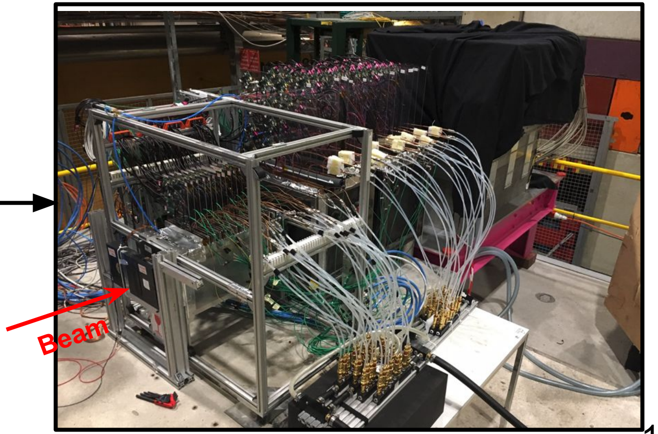

Beam test setup in October 2018

See [link] for more details

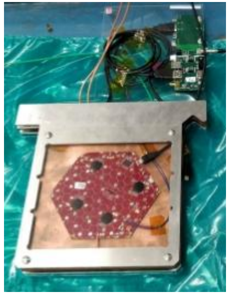

EM section: CE-E prototype

- Hanging file structure
- 28 sampling layer
- 14 double sided mini-cassettes
- **Pb/Cu/CuW absorber**
- **~ 28 X_0, 1.4 λ_{int}**

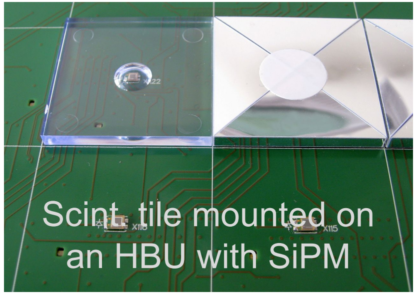

Had section: CALICE AHCAL prototype

- Scintillator-on-SiPM
- 39 sampling layers
- **Steel absorber**
- **~ 4.4 λ_{int}**

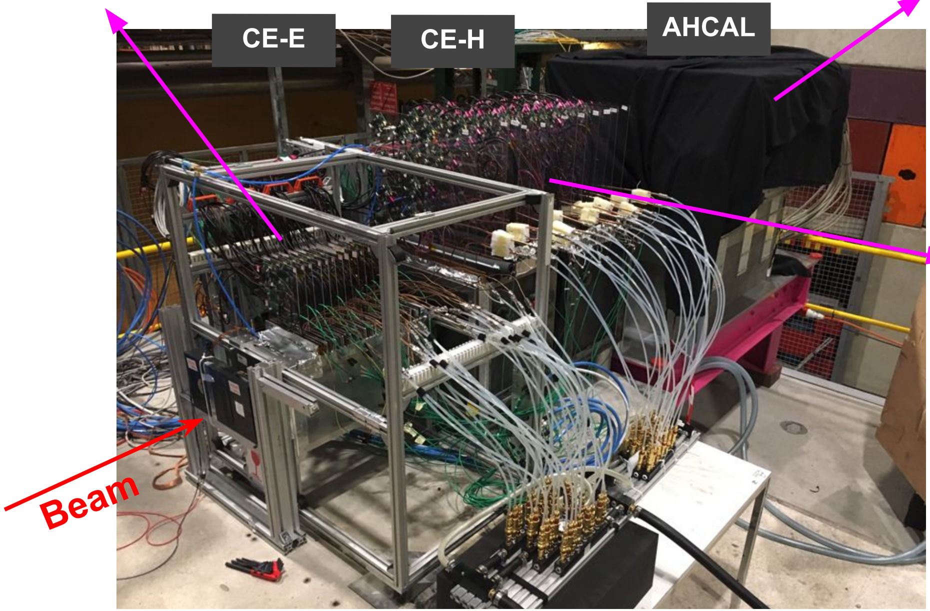

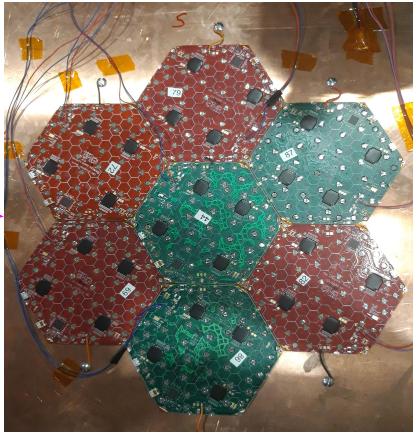

Had section: CE-H prototype

- Hanging file structure
- 12 sampling layers
- Modules arranged in daisy structure
- **Steel absorber**
- **~ 3.4 λ_{int}**

Si HGCAL protype: 94 sensor modules, ~12K channels
Scint AHCAL prototype ~22K channels

The setup was exposed to $\boldsymbol{e^+}$, $\boldsymbol{\pi^-}$ beam of energies ranging from 20 to 300 GeV and 200 GeV $\boldsymbol{\mu^-}$ beams.

Particle beam for beam test experiment

- Beam test experiment performed at North Area Facility in Prevessin, CERN.
- 400 GeV proton beam from SPS interacts with fixed target → produces secondary particle beam.
- Secondary particle beam is selected & focused with the help of beam optics:
  - Collimeters, dipole & quadrupole magnets etc.
- The beam is transported to experimental halls via beamlines.
  - HGCAL beam test was held at H2 beamline

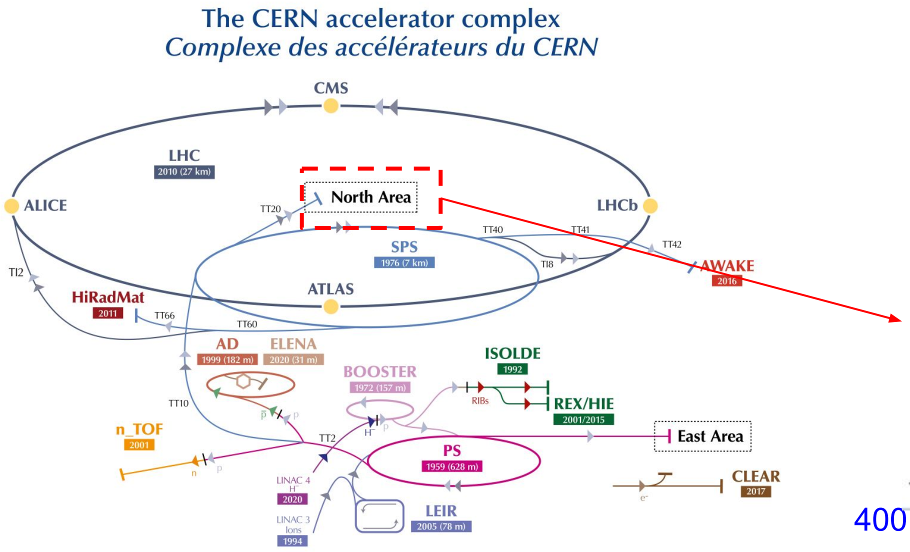

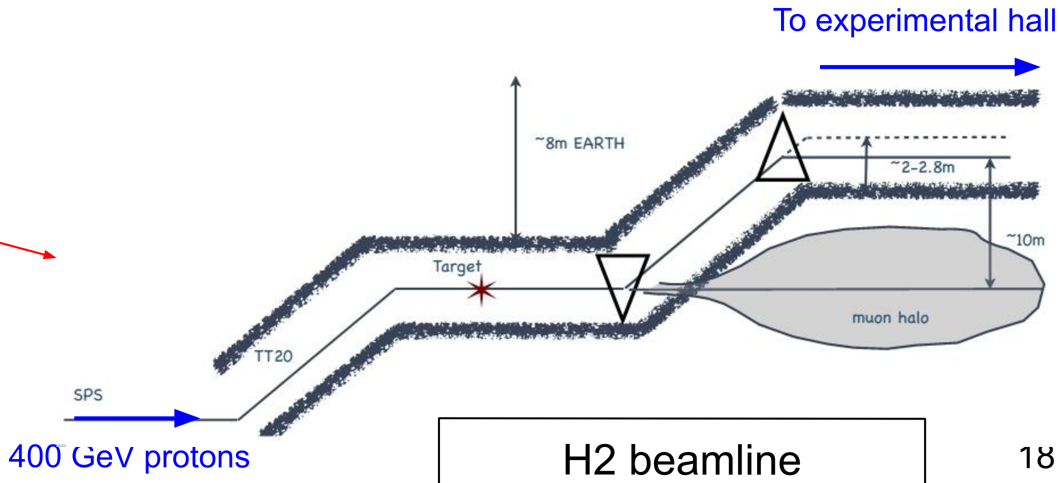

Beamline detectors

Apart from HGCAL and AHCAL detector prototype, various detectors were deployed upstream the experimental setup to help in data taking operation & data analysis.

Cherenkov (XCET)
- For particle identification
- very low efficiency (<1%)
- Not used in any analysis

Scintillators
- To generate triggers for data taking
- Coincidence and veto triggering

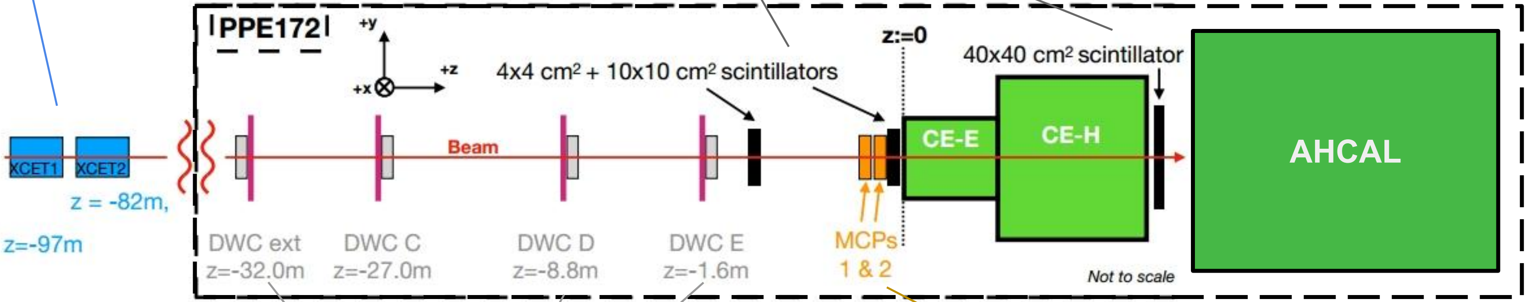

Delay wire chambers (DWC)
- For track reconstruction.

Micro channel plate (MCP)
- For timing reference.

Detector set up in GEANT4 simulation

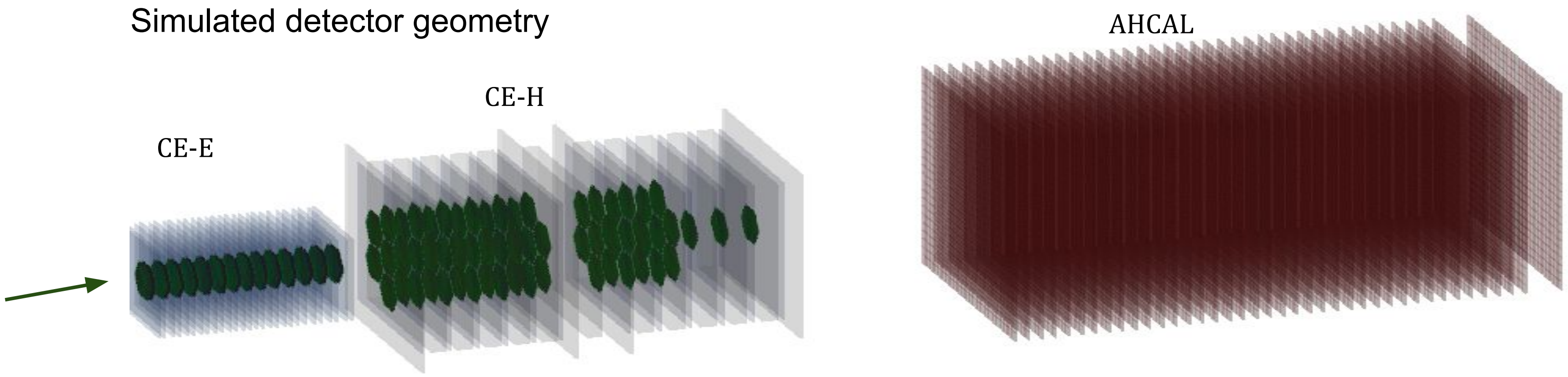

- Different sampling fractions CE-E, CE-H and AHCAL :
  - CE-E: 1.4 λ_{int} & $\Delta\lambda_{int}$~ 0.05 λ_{int}
  - CE-H: 3.4 λ_{in} & $\Delta\lambda_{int}$~ 0.3 λ_{int}
  - AHCAL: 4.4 λ_{in} & $\Delta\lambda_{int}$ ~ 0.1 λ_{int}
- The H2 beamline elements (quadrupoles, dipoles, collimators, other detectors) are simulated using G4Beamline package.
  - Important for e+: synchrotron radiation.
- Energies: 20, 50, 80, 100, 120, 200, 250, 300 GeV

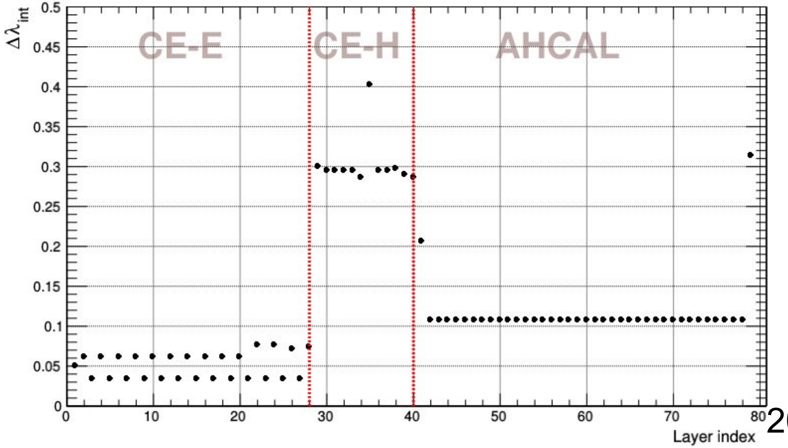

Study of the performance of CMS HGCAL detector prototype

More than 6 million events were recorded over a span of three weeks of data taking.

Goals:

- ➔ Proof-of-concept of large scale prototype
- ➔ Test readout electronics
- ➔ Signal-to-noise ratio of Si sensors
- ➔ Performance to Electromagnetic showers
- ➔ Performance to Hadronic showers
- ➔ Timing performance.
- ➔ Simulation modelling

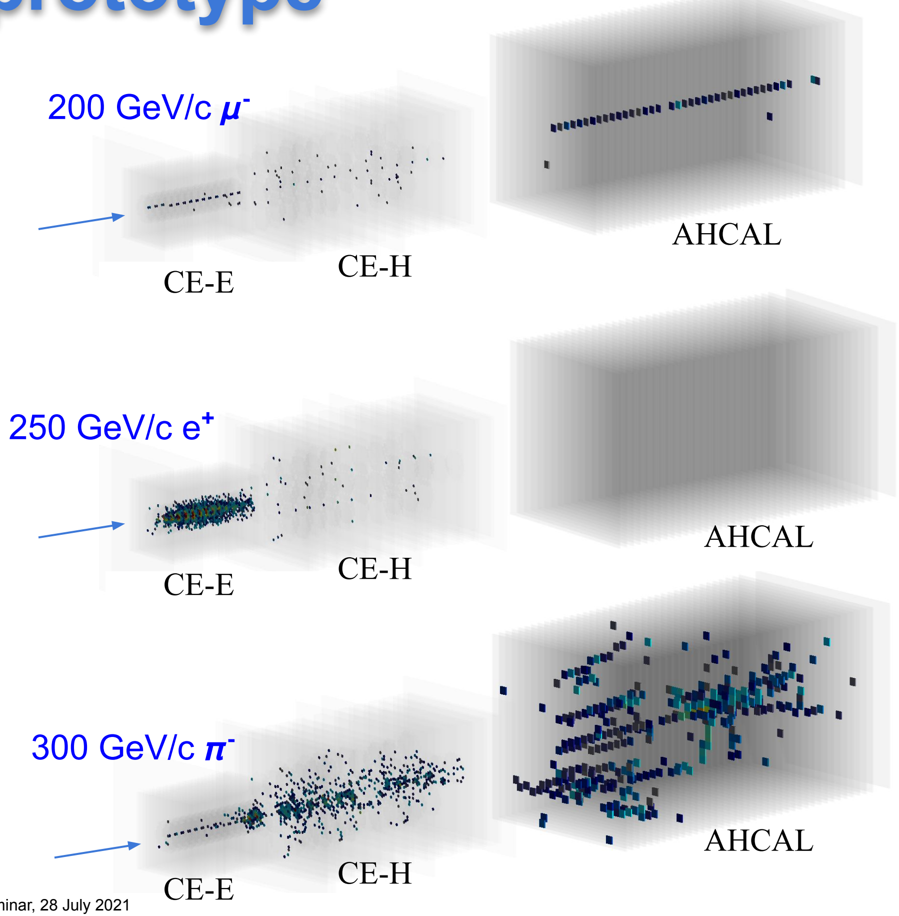

Intergain Calibration

- **SkiRoc2-CMS ASIC**: different ADC gain stages (High Gain/Low Gain) and Time-over-Threshold (ToT).
  - Allows a wide dynamic range of energy measurement.

- To ensure a linear response over a large dynamic range, gain intercalibration is performed.

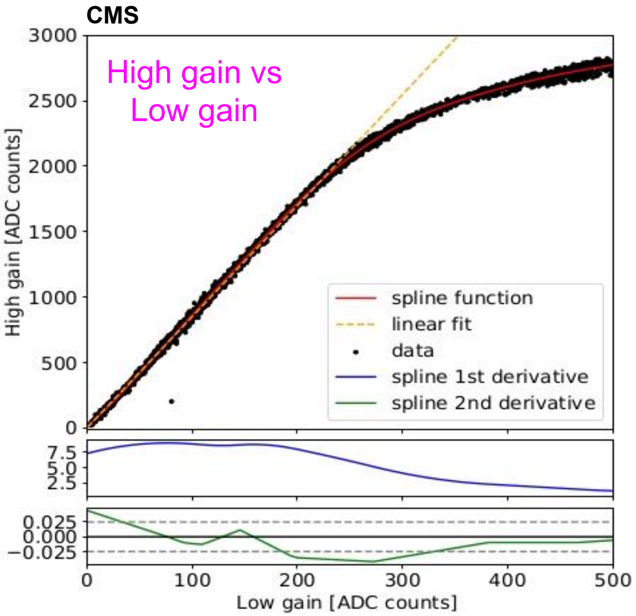

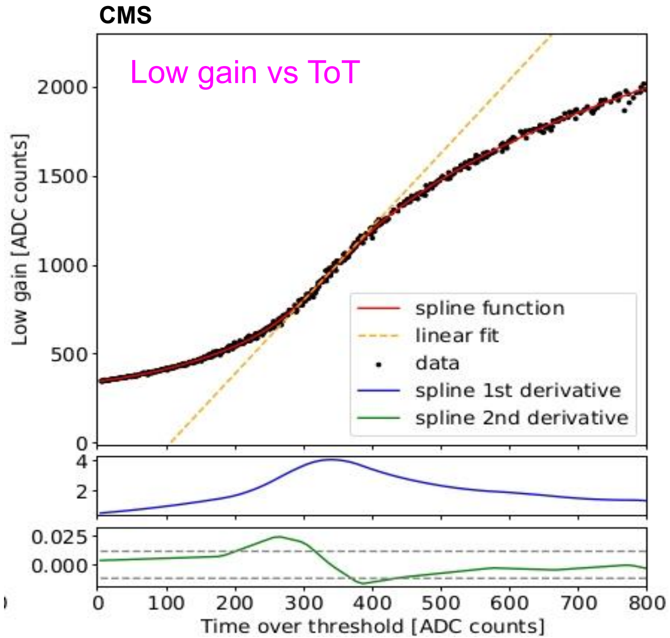

Sufficient overlap between gains: Fit straight line in the linear region → obtain fit coeff. [intergain calib. factors]

Channel-to-channel response equalization

- Different cells may have diff. response to identical traversing particle.
  - Differences in actual depletion widths
  - Differences in gain settings of ASICs

- Equalize response with minimum-ionizing-particles (MIPs)
  - 200 GeV/c μ^- beam → proxy for MIPs
  - Fit ADC distribution → Landau convoluted with Gaussian.
  - Extract the MIP peak as calibration constant.

- Overall ~85% Si cells calibrated in CE-E & CE-H.

- Estimate **signal-to-noise ratio** of Si cells:
  - Level of separation b/w signal and inherent noise in Si cells.
  - Important input for future sensor module designs.

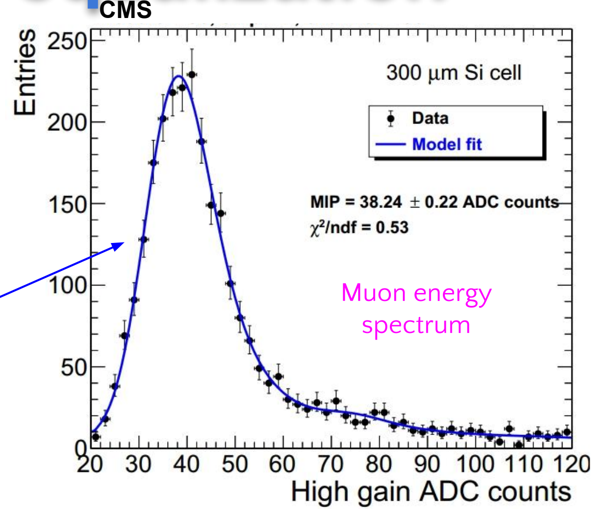

Muon energy spectrum

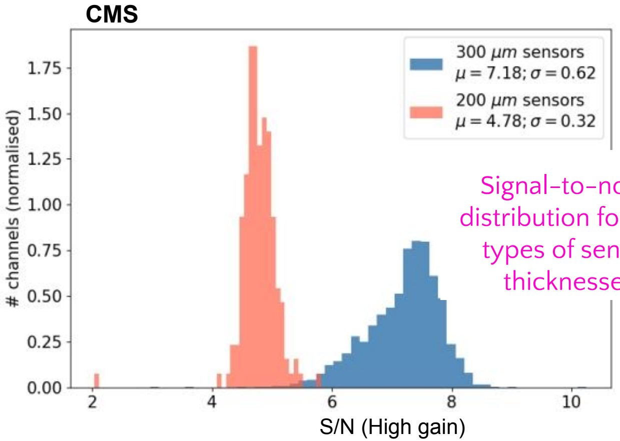

Signal-to-noise distribution for two types of sensor thicknesses

Using channel-to-channel and intergain calibration factors, the energy is reconstructed in **MIP equivalent** of energy deposit for each hit.

Physics performance to EM showers

Beam test experimental setup was exposed to positron (e^+) beam with energies ranging from 20 to 300 GeV.

Example event display
October 2018 TB: **Run 646 - event 2**
250 GeV positron

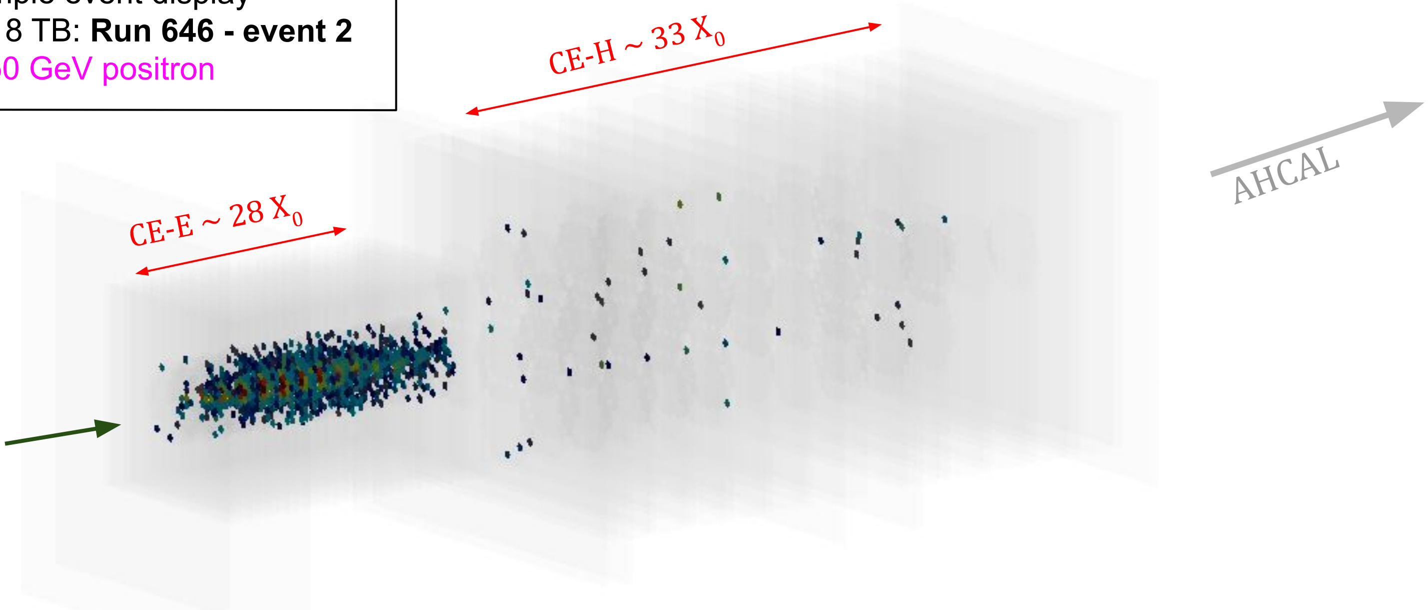

Energy linearity and resolution of EM showers

Energy of EM shower is reconstructed with the shower energy deposited in CE-E prototype.

CMS preliminary

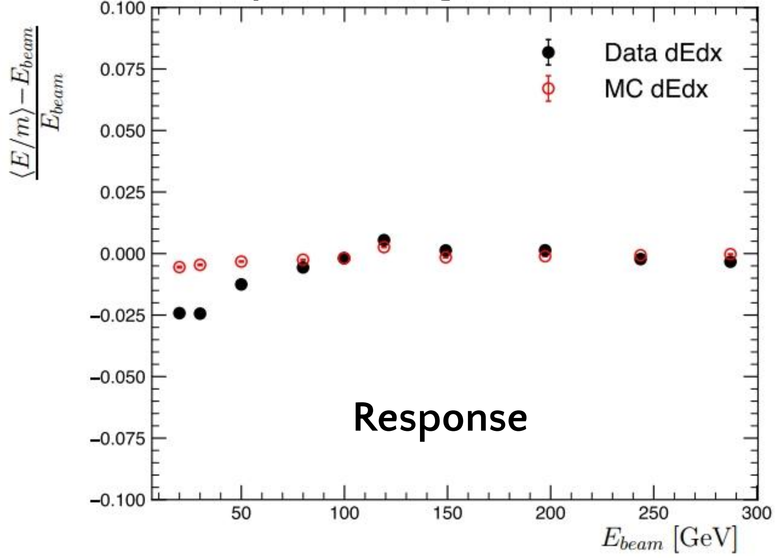

- ➢ Linear response → As expected.
- ➢ Agreement within ~ 2.5% between data & MC.

CMS preliminary

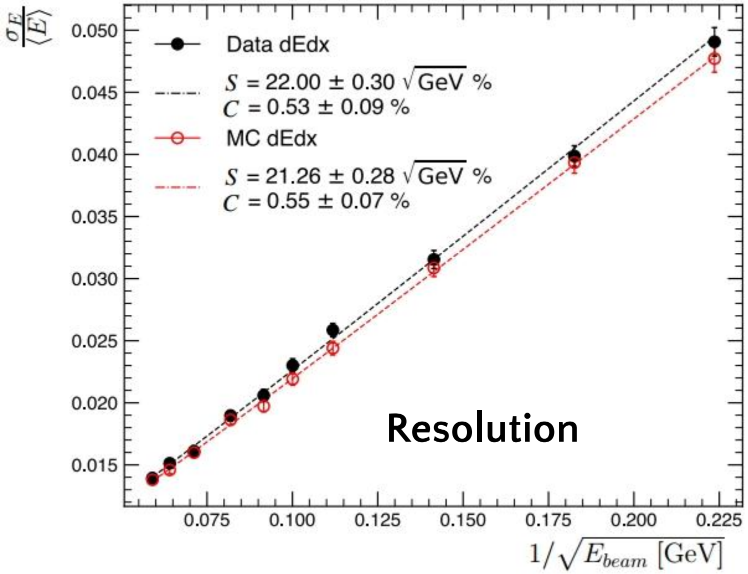

- ➢ Stochastic terms ~ 22% → close to final design (~20%)
- ➢ Good agreement between data and MC.

EM longitudinal shower development

Median energy deposited [MIPs] as a function of calorimeter depth (CE-E).

CMS preliminary

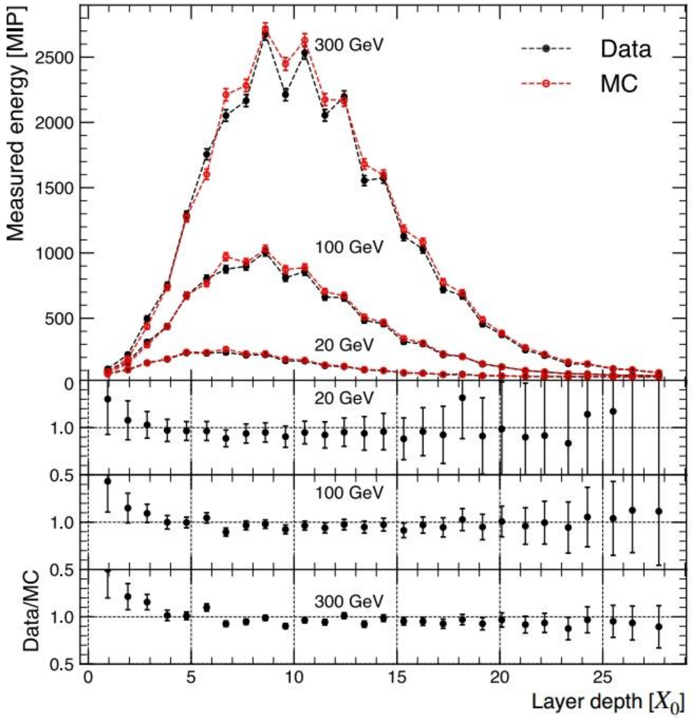

Obtain shower maxima by fitting **Longo's parametrization**

CMS preliminary

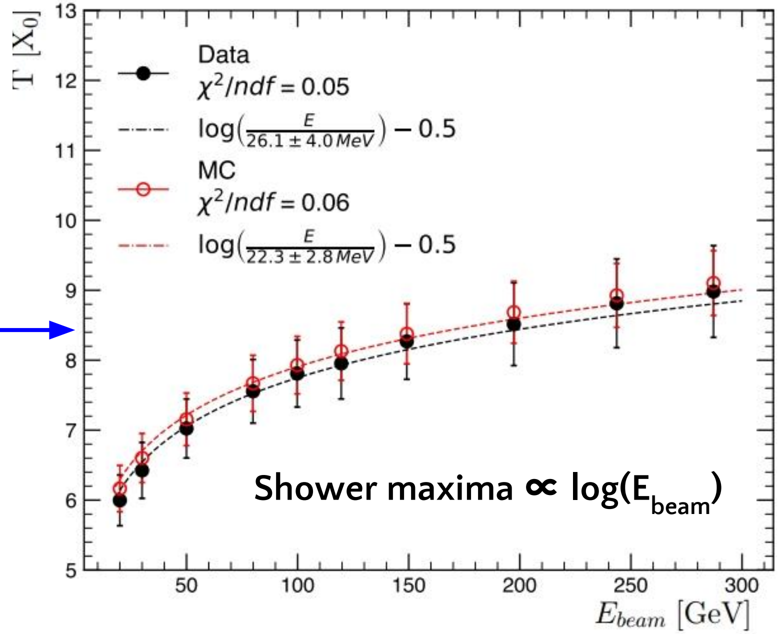

Simulation reproduces EM shower development very well.

Physics performance to hadronic showers

π^- beam $\in$ [20, 300] GeV

In collaboration with ILC CALICE

Depth of first hadronic interaction

(Shower start finder algorithm)

High granularity of CE-E and CE-H prototype allows us to develop an algorithm to identify the location of first hadronic interaction of pion where it initiates showering.

Example event display
October 2018 TB: **Run 515 - event 12**
300 GeV pion

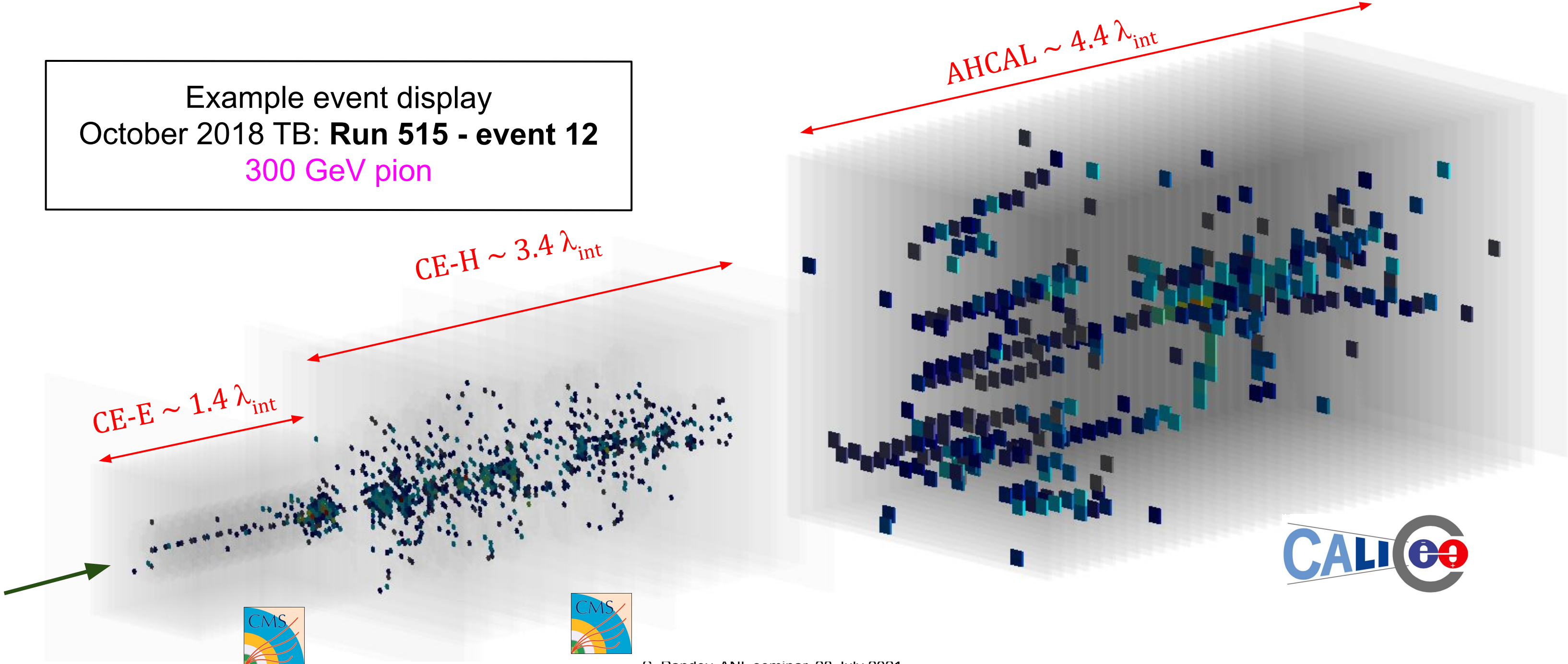

Shower start finder algorithm

- Development and optimization done with the truth information from Geant4 simulation.
  - Hit multiplicity, energy deposition & lateral spread pattern in consecutive active layers.

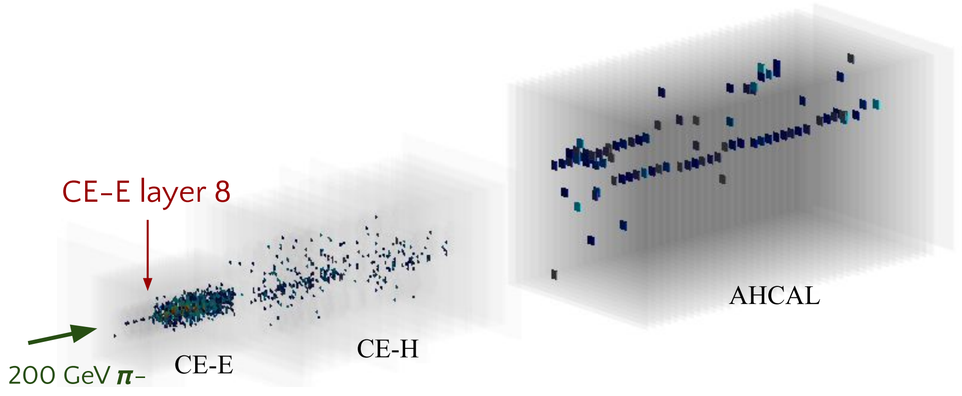

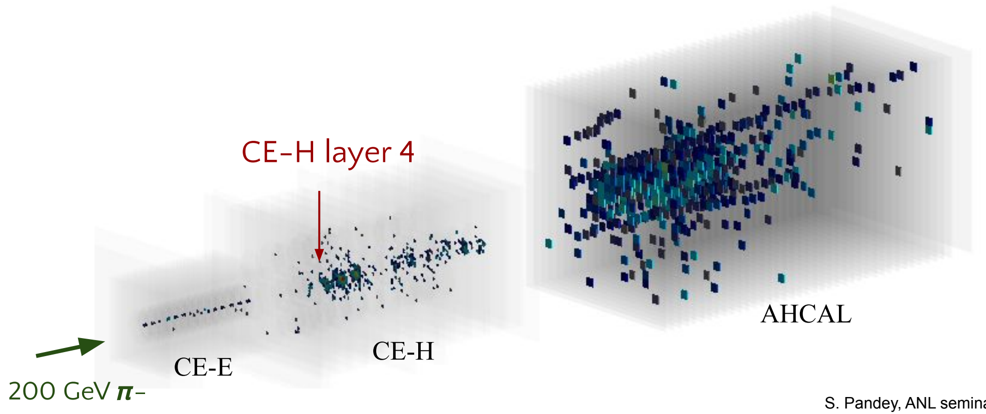

Shower start location as a function of calo. depth

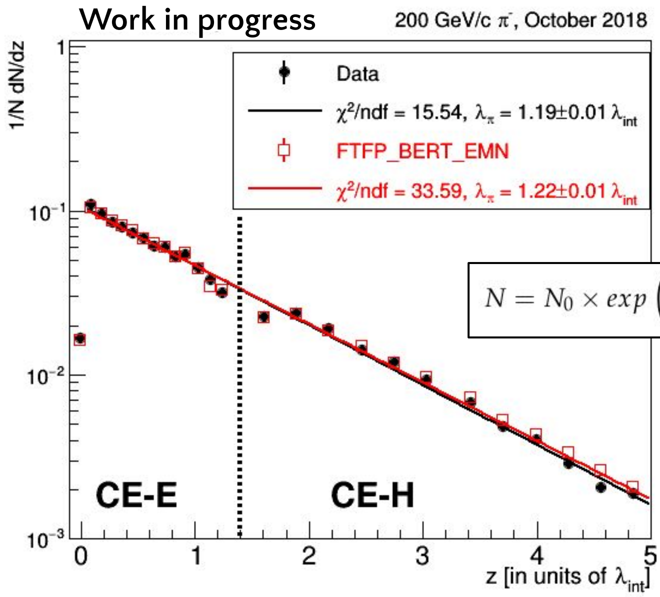

$$N = N_0 \times exp\left(\frac{-z}{\lambda_{int}}\right)$$

Exponential falling behaviour and good agreement between data-MC

Energy reconstruction of pions

- Energy deposited by pion showers, is shared between the electromagnetic and hadronic sections.

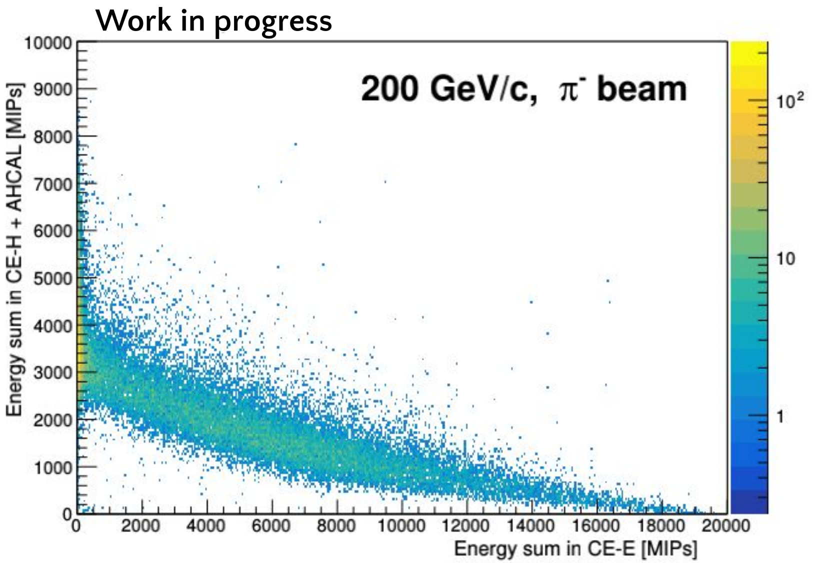

Sum up the energies →

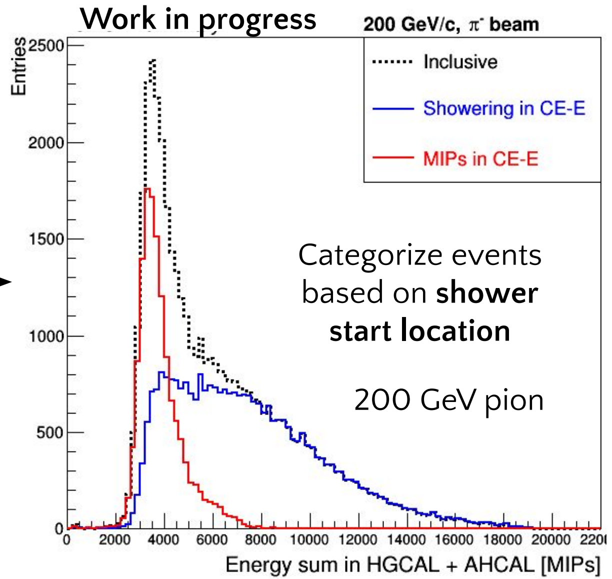

- Different sampling fractions for the two sections → Just summing up the energies is not the right way !!!
- Optimally combine the energies from different sections:
  - Simplest way : Use calorimeter based calibration i.e. use **50 GeV e^+** to set MIP-to-GeV energy scale for CE-E and **50 GeV *π*-** to set MIP-to-GeV energy scale for CE-H & AHCAL.

Energy response [with calo. calibration]

- Combine the energies with calorimeter based MIP-to-GeV scale → fixed weights.
  - EM section (CE) : **10.6 MeV per MIP** [using 50 GeV e+ beam]
  - Had section (CH + AHCAL) : **78.9 MeV per MIP** [using 50 GeV pi- beam, MIPs in CE-E]
    - CE-H & AHCAL also have different sampling fraction → constant relative-weight = 0.4

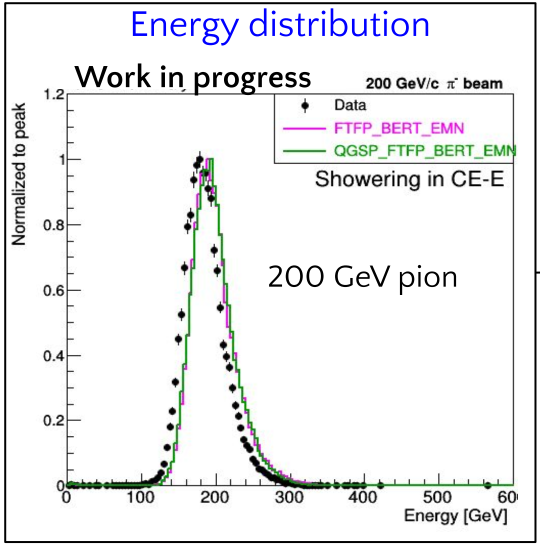

Fit a gaussian function to obtain response: μ_{gaus}/E_{beam}

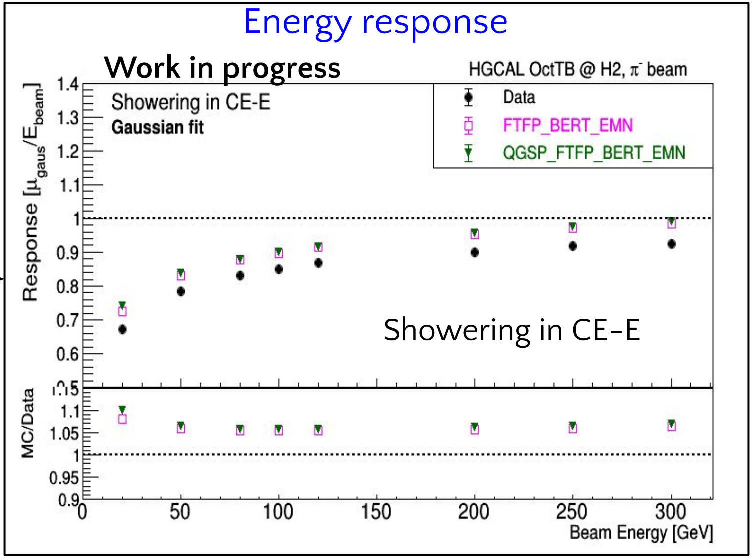

- ➔ The energy distribution shape is reproduced well by simulation.
- ➔ Non-linear energy response → non-compensating calorimeter (e/h > 1).
- ➔ Flat energy scale difference between data and MC → apply a global factor on MC to match the scale.

χ^2 optimization of weights

- Energy response can be linearized : energy-dependent weights
- For pions showering in CE-E (EH pions):

$$E^{corr}\,[\text{in GeV}] = \alpha_1(E_{beam}) * E^{CE\text{-}E}_{fix} + \beta_1(E_{beam}) * E^{CE\text{-}H}_{fix} + \gamma_1(E_{beam}) * E^{AH}_{fix}$$

- Construct and minimize $\chi 2$ analytically:

$$\chi^2 = \sum_{pions} \frac{(E_{beam} - E^{EH}_{corr})^2}{\sigma^2(E)}$$

  - CE-E/CE-H/AHCAL energy is already set to GeV (fixed weights).
  - σ(E) is the uncertainty in the measured energy (fixed-weights).

- **The weights are determined using TB data** and are applied on both data and simulation.

- In the real experiment, track momenta is taken as a reference to extract energy-dependent weights.
  - For neutral hadrons or beyond tracker coverage, calo. energy measured using fixed weights (method-1) is taken as a reference.
  - We fit the weights with a polynomial function, and evaluate the weights from the fitted function.

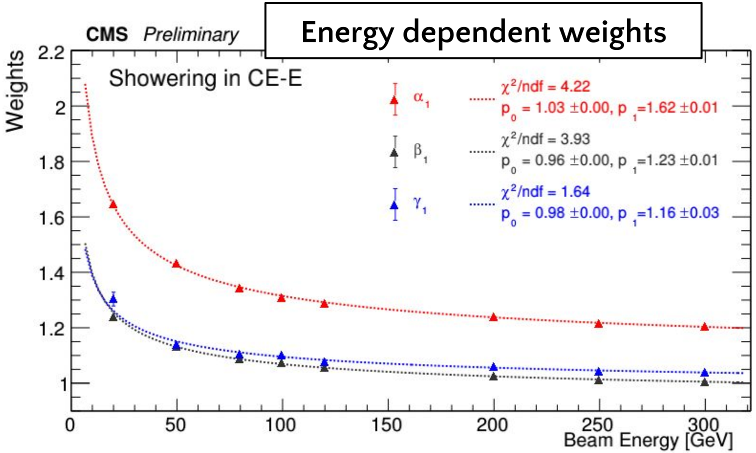

Response and resolution data-MC comparison

Response and resolution comparison in data-MC after applying optimized weights.
(**Energy rescaling has been applied on MC to match data.**)

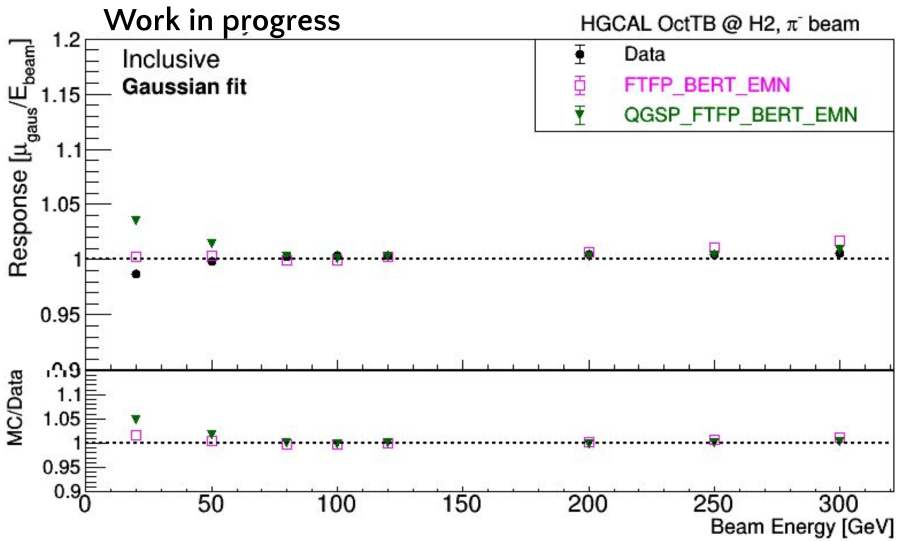

Response

- ~ Linear response with energy dep. weights.
- Agreement within ~ 5% between data & MC.

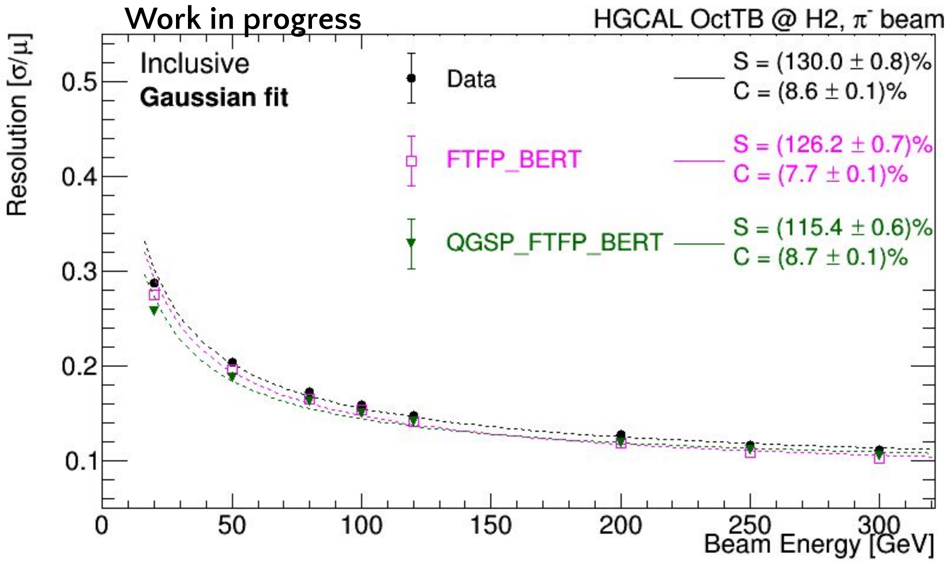

Resolution

- Better agreement at higher energies & slight difference at lower energies.
- Overall agreement 5 - 10% at low energies .

Shower development comparisons in data-MC

Longitudinal shower shape

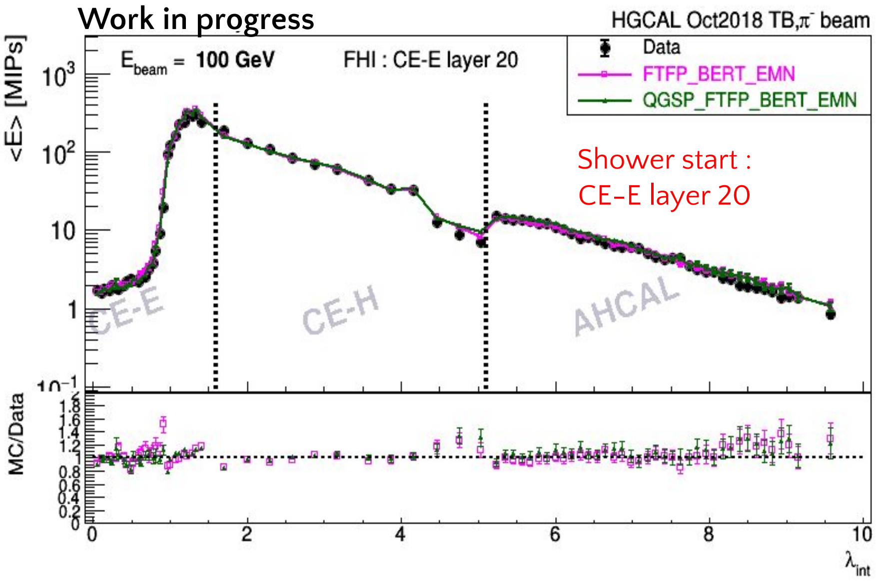

Mean energy deposited (in MIPs) as a function of calo. depth (λ_{int}) for different shower start location.

Transverse shower shape

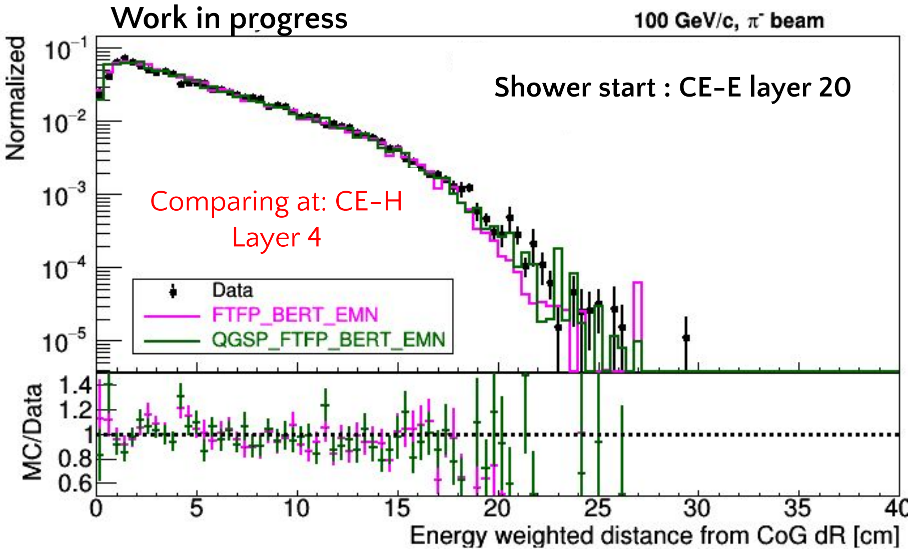

Energy weighted distance ($dR^{weighted}$) from the center of gravity at layers downstream of shower start location.

Shower development is reasonably well reproduced by simulation.

Summary

- **HL-LHC** → opportunity for finding new physics in direct searches as well as testing the limits of SM.
- **Challenges for detectors** → Upgrade studies (with real data & MC) are in full swing.
- CMS HGCAL group performed beam test experiment in collab. with ILC CALICE group during october 2018.

Goals: Proof-of-concept ✓

- ➔ Test readout electronics
- ➔ Signal-to-noise ratio of Si sensors
  → The DAQ system for HGCAL prototype: 2021 JINST 16 T04001
  → Construction and commissioning of CMS CE prototype: 2021 JINST 16 T04002
- ➔ Performance to Electromagnetic showers → Paper draft already under review with editorial board.
- ➔ Performance to Hadronic showers → Results are being finalized and paper is under preparation.
- ➔ Timing performance → Being analyzed : will be published as a separate paper.
- ➔ Simulation modelling ✓

What's next??

Sensor prototype moving closer to final design:

➔ 8" modules
➔ Close to final ASIC design : HGCROC

Prototype testing:

➔ Test in lab benches
➔ Planned beam test this September/November at SPS CERN
➔ Thorough testing of prototypes

Module Assembly Centers:

➔ For large scale production
➔ Five centers around the world: UCSB (CA) pilot

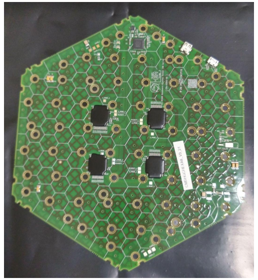

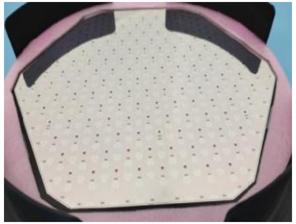

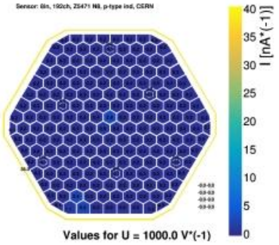

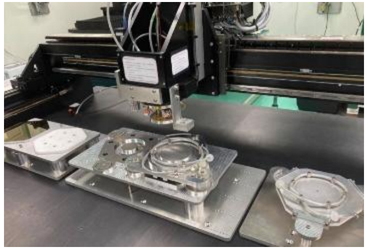

Get the detector ready for physics data taking !!!

Thank you

BACKUP

High Luminosity Large Hadron Collider (HL-LHC)

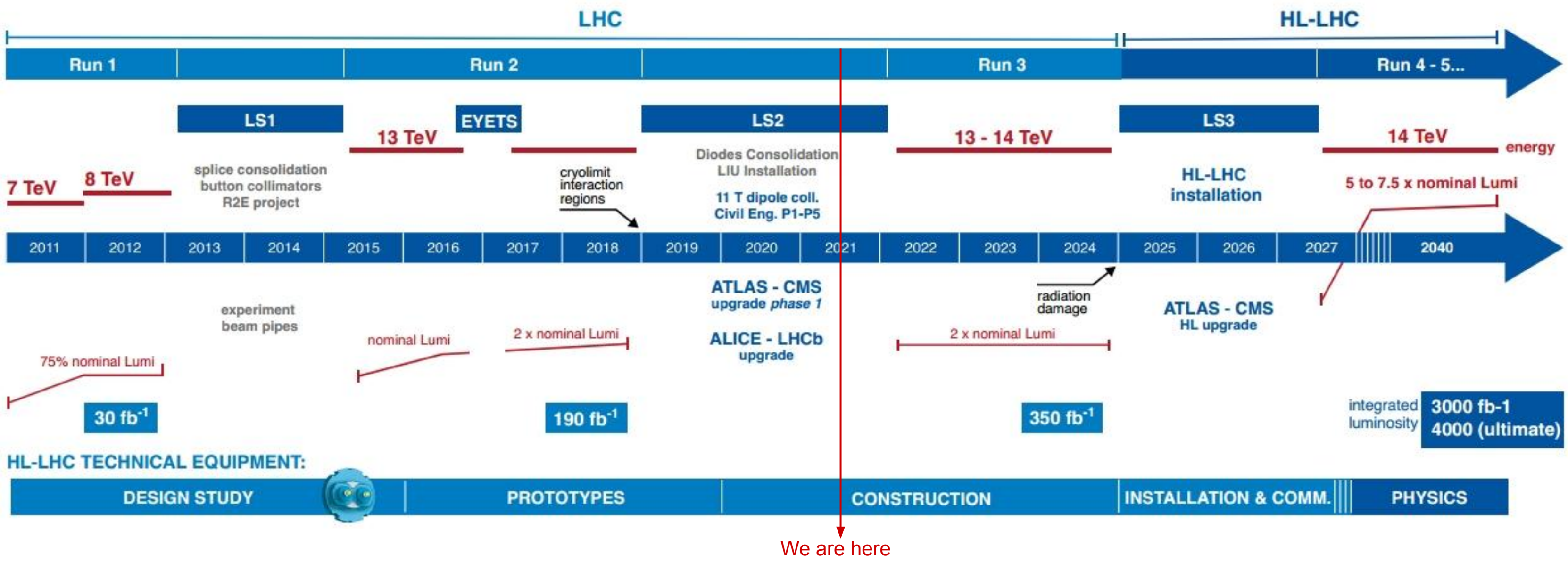

HL-LHC run is expected to start around 2027.

HL-LHC will deliver 10x more integrated luminosity than LHC over 10 years of operation.

Advantages

More Statistics for:

- Higgs and other SM precision measurements
- Searches for Beyond SM physics

Challenges

- Very high radiation dose
- High pile-up condition
    - <PU> ~ 140 - 200 per bunch collision

Physics opportunities at HL-LHC

Improvement in precision measurement

Higgs boson coupling as a function of boson/fermion masses

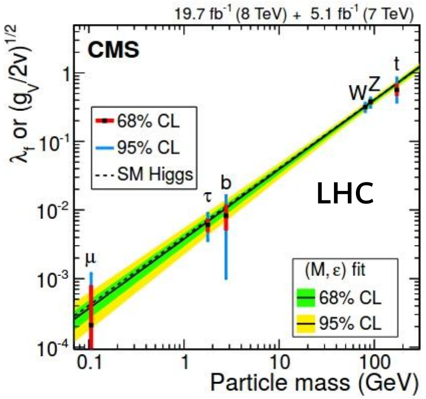

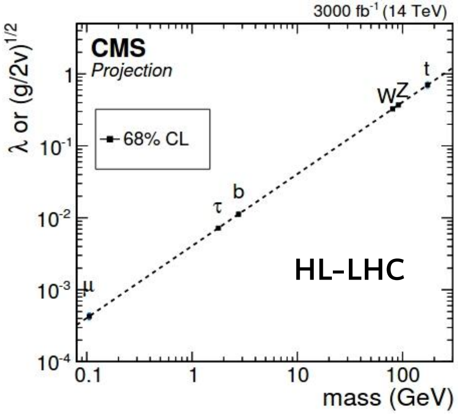

Reduced uncertainty

Scope of direct searches of new physics

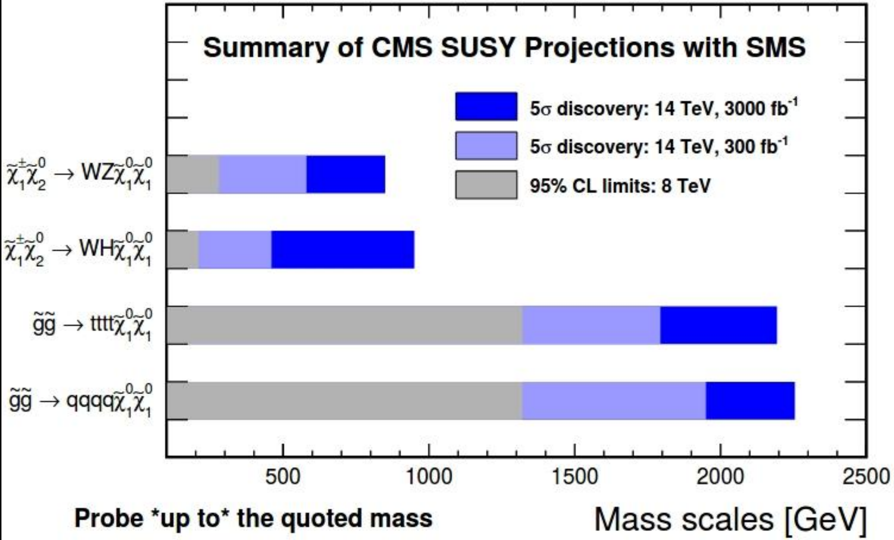

Probe *up to* the quoted mass

Other physics opportunities:

- Beyond 3.5σ significance for H → di-muon pair
- Measurement of di-higgs production with σ ~ 40 fb
- Access to small cross sections for other new physics such as dark matter.

Particle flow: general

- Identify and reconstruct all constituents in the event before performing any jet clustering → optimizing the detector performance.
  - Electrons, photons, charged and neutral hadrons, muons.
  - Take advantage of excellent tracking whenever possible.

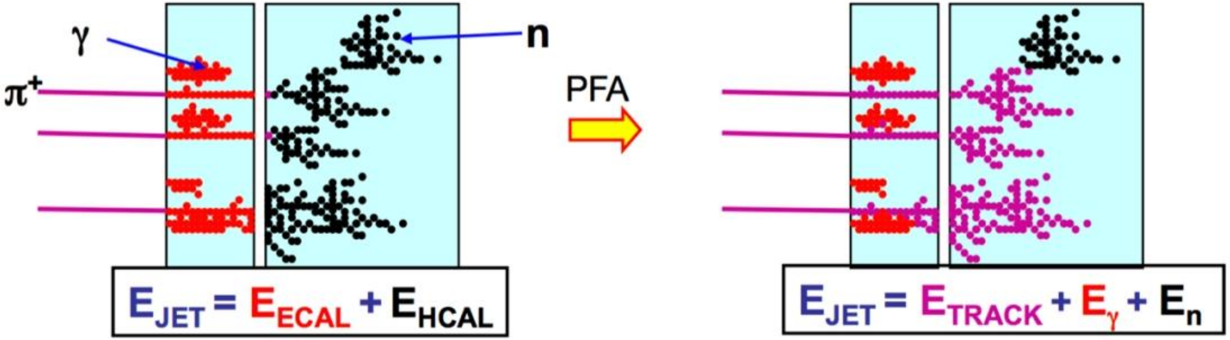

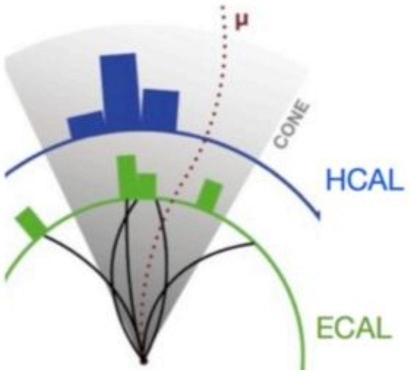

Jet Constituents

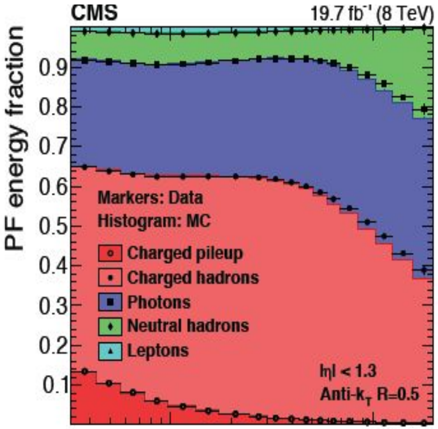

Particle flow technique: Improvements

Improvement in both response as well as resolution compared to "only" calorimeter information.

Response as a function of η

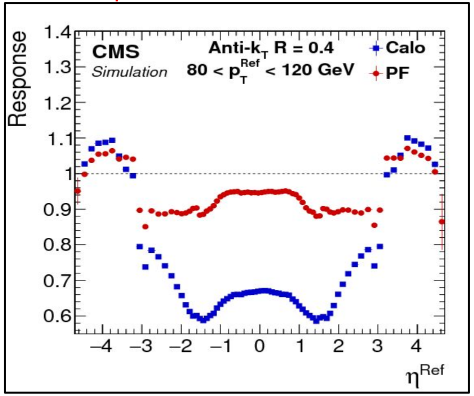

Response as a function of p_T

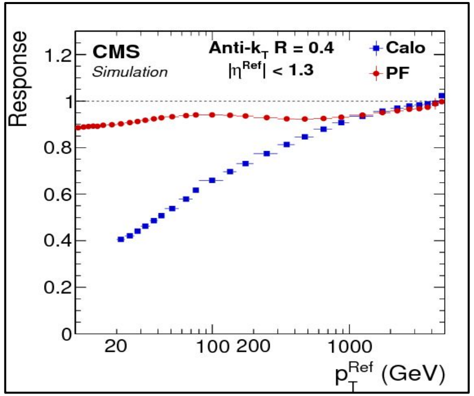

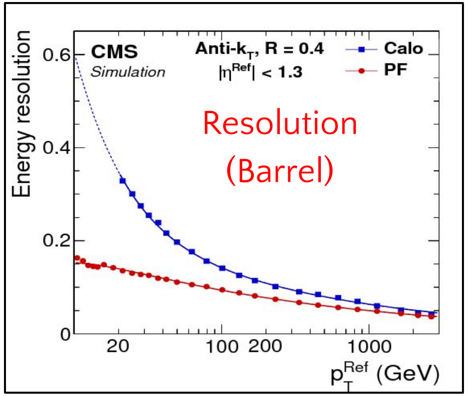

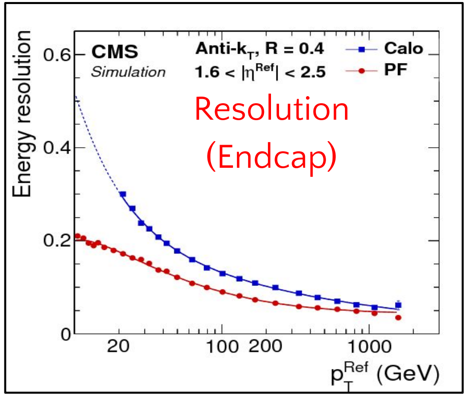

VBF H→ γγ event display in HGCAL (simulated)

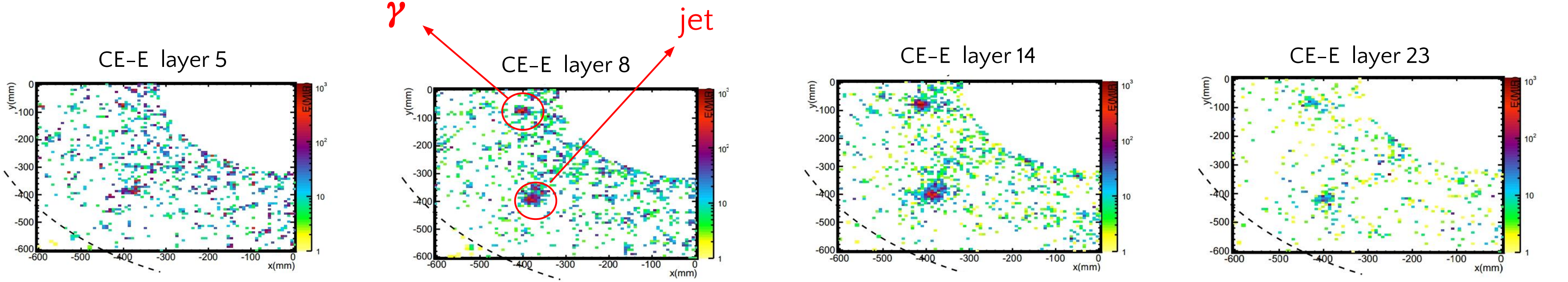

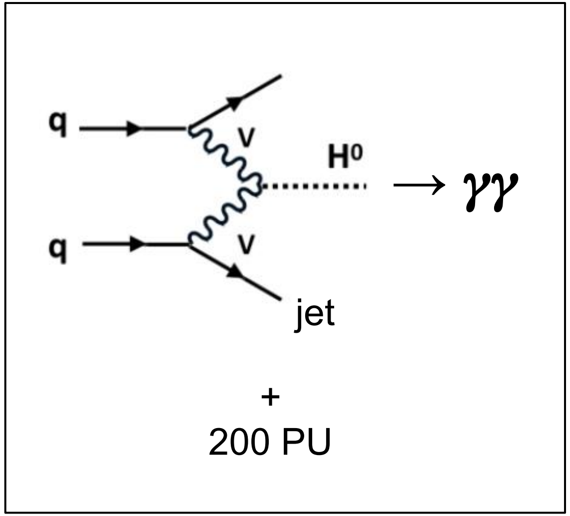

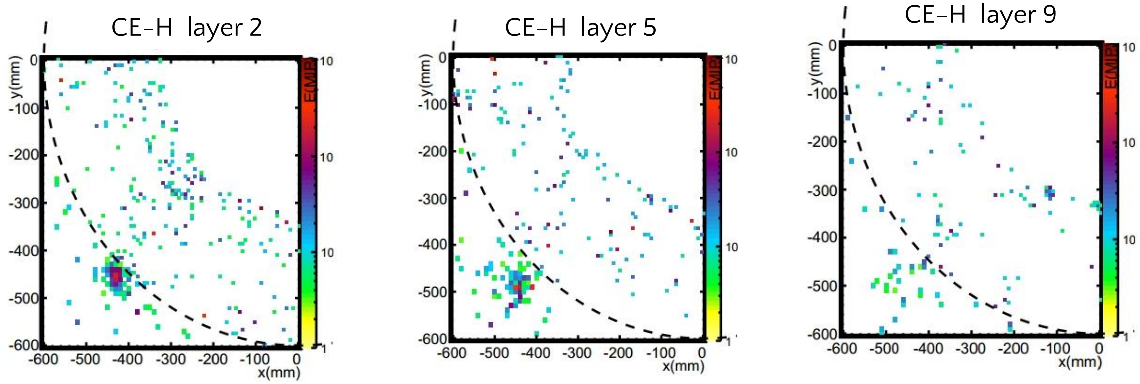

Showers visible in the EM & Had layers of HGCAL

Timing capability : PU mitigation

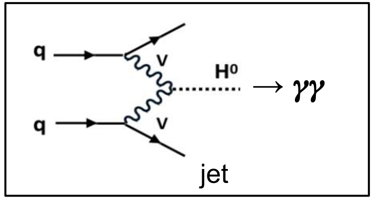

VBF (H → γγ) event with one γ and VBF jet in the same quadrant.
Image projected onto the front face of HGCAL.

Without any timing requirement.

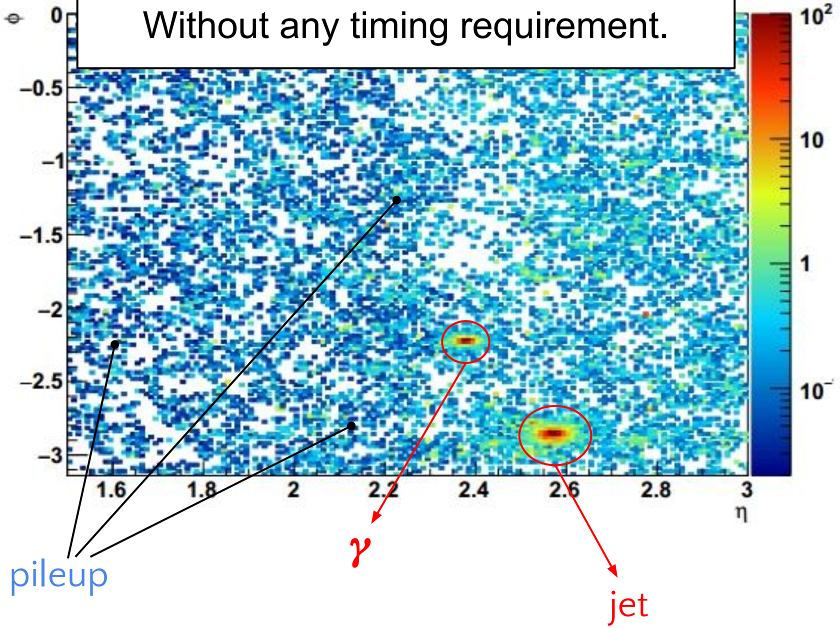

Cut |Δt| < 90ps on cells with q > 12fC

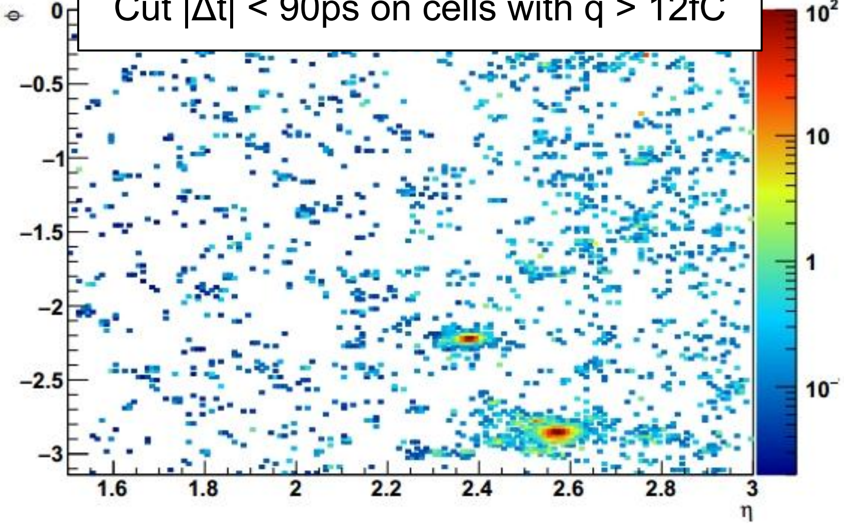

Silicon sensor thicknesses

Studies show for increasing irradiation, "decrease" in charge collection is lesser for thinner sensors as compared to thicker sensors.

↓

Use thinner silicon sensors at higher η i.e. more fluence region.

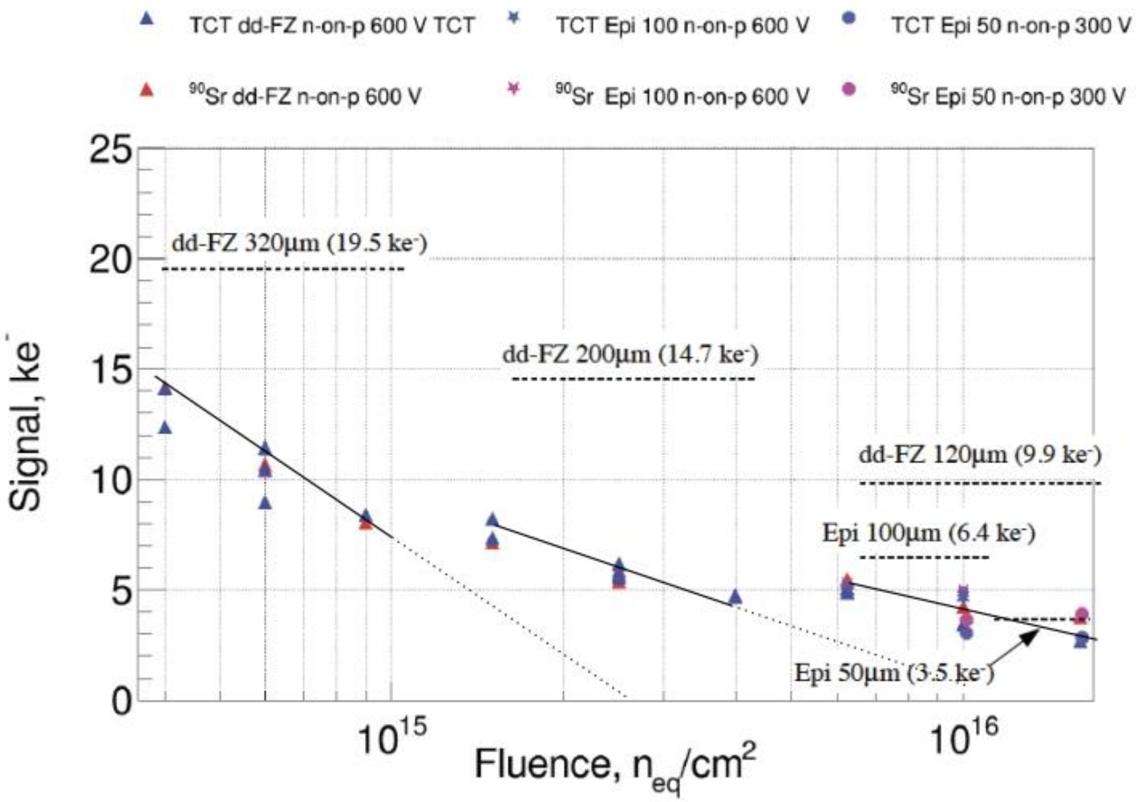

DAQ system for v2016 module

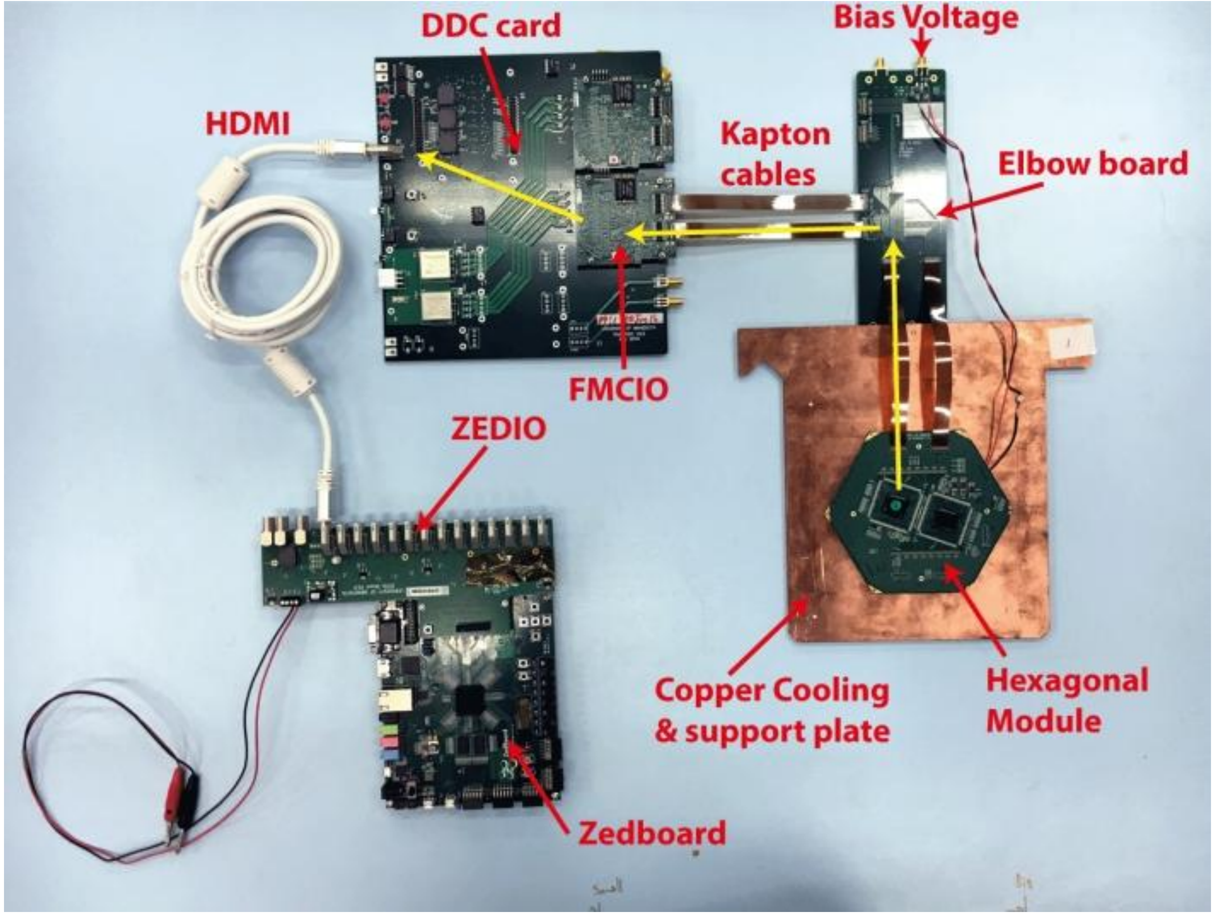

Trigger Flow

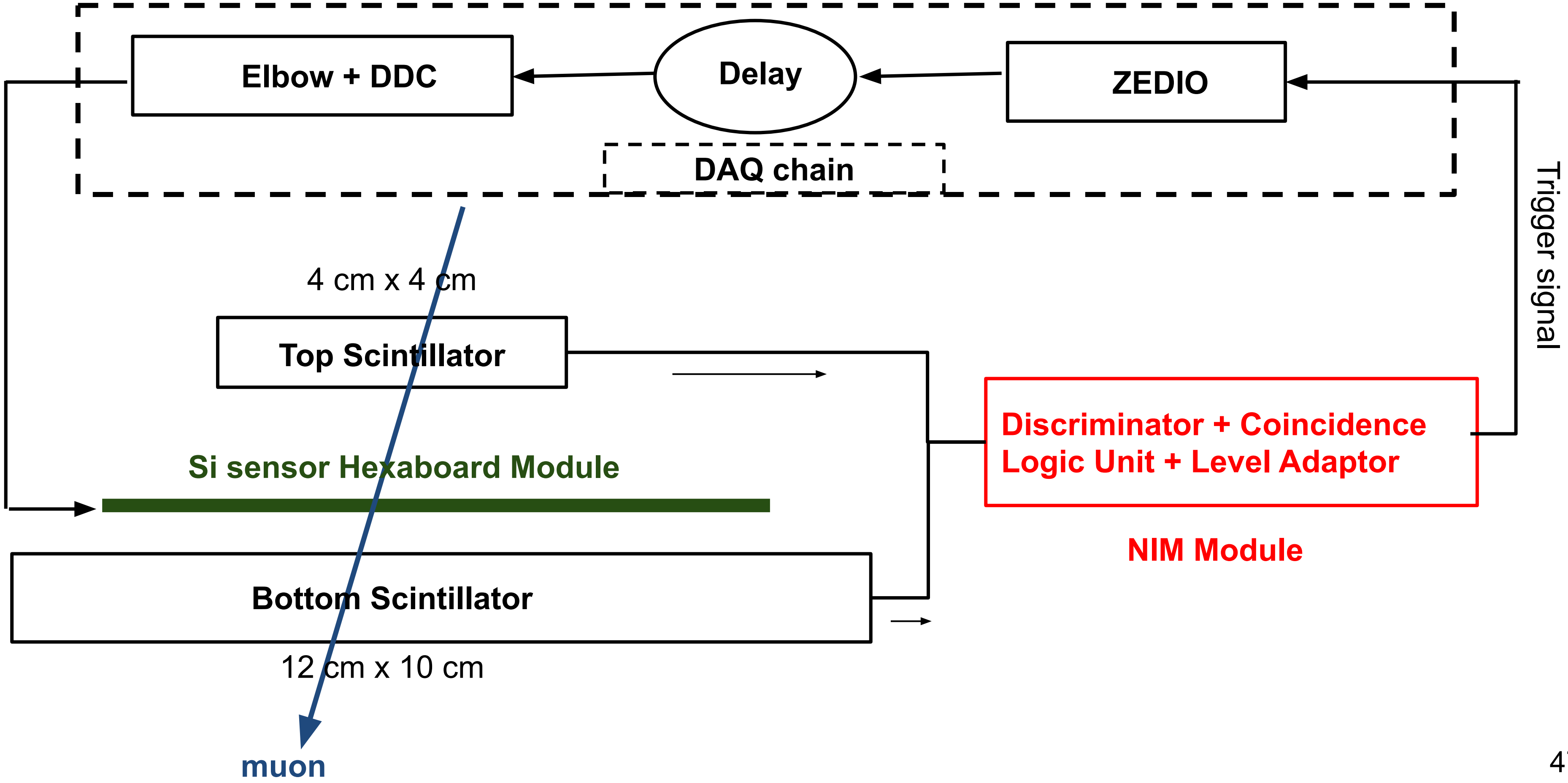

SkiROC2-CMS ASIC

- SkiROC2-CMS ASIC is a readout chip, designed for digitization of charge collected by silicon sensor.
- Each chip has 64 channels and each channel provides a pre-amplifier, two pulse-shapers, 13-deep analog memory, analog-to-digital converter and two timing measurements (Time-over-Threshold & Time-of-Arrival).
- It can measure signals ranging from a few fC to 10 pC, hence provides a large dynamic range for energy measurement.

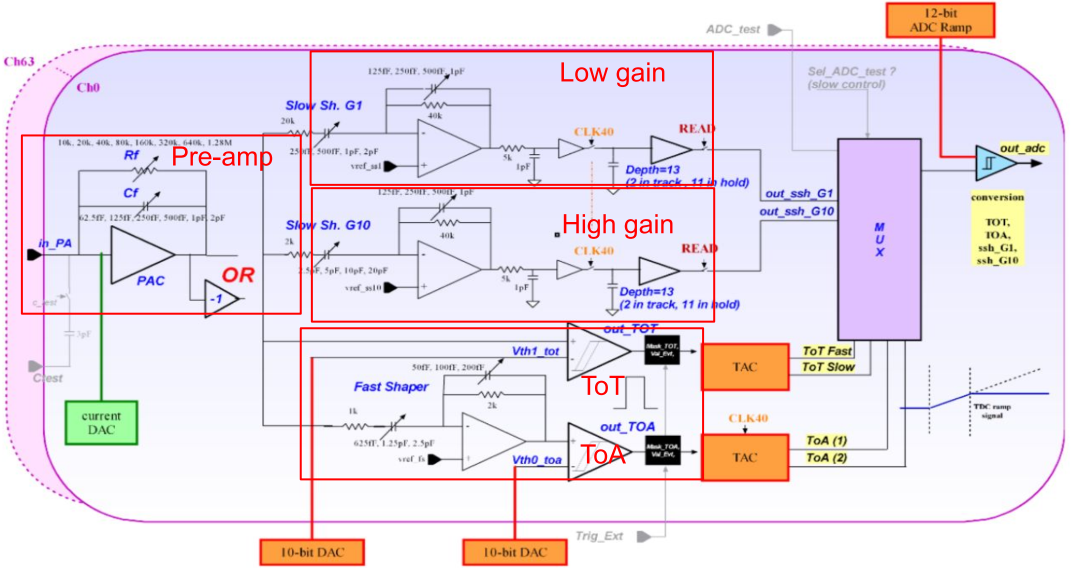

SkiROC2-CMS Schematic Diagram

Following ADC data is read out when a trigger is supplied to the chip:
- ADC counts from **high-gain shaper** in 13 time-samples*.
- ADC counts from **low-gain shaper** in 13 time-samples*.
- one Time-over-Threshold and one Time-of-Arrival ADC data.

*Each time sample corresponds to integrated charge in 25nS wide time-window.

Signal to noise ratio estimation

- For Si sensors in HGCAL prototype, we define S/N ratio as the ratio of:
    - Signal produced by MIP (HG ADC counts per MIP) and
    - Noise level in the absence of ionizing particle i.e. fluctuation about zero in HG ADC count distribution.

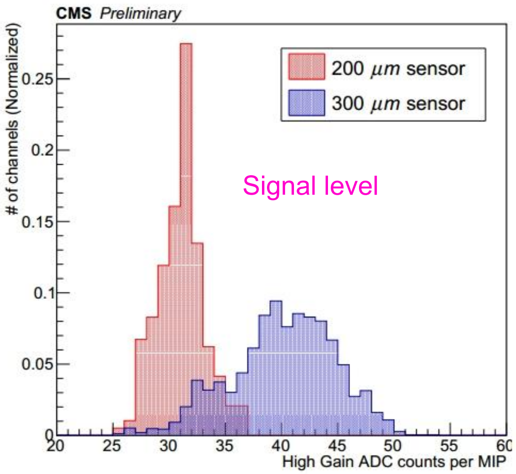

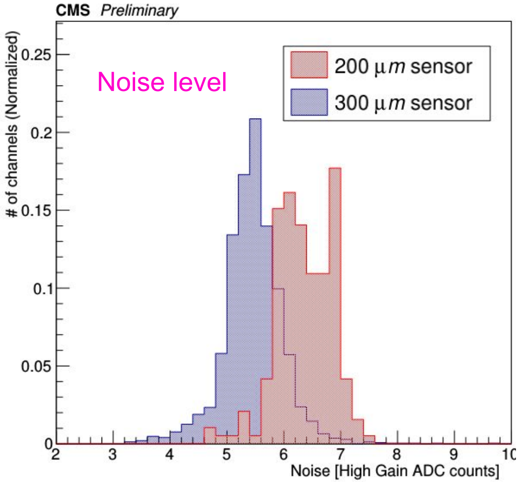

- More charge collected in 300 μm as compared to 200 μm si cell
- High signal in 300 μm than 200 μm si cell

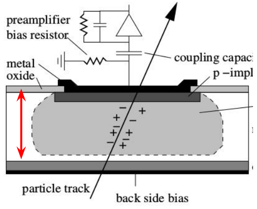

$$C = \frac{\epsilon A}{W}$$

Capacitance

$$Z_C = \frac{1}{2\pi f C}$$

Impedance

Smaller active width → Higher cell capacitance → Higher noise

S/N estimation and result

- Now that we have estimated signal level (MIP signal) and noise level, it is straightforward to calculate S/N ratio.
  - Similar procedure is followed for low gain channels as well.

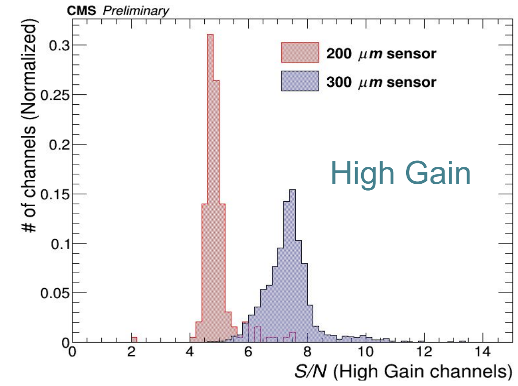

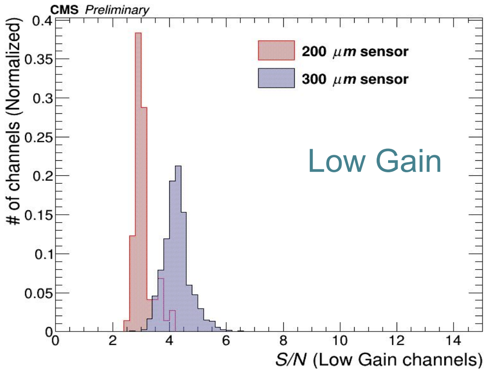

300 μm Si cell have better S/N ratio as compared to 200 μm cells.

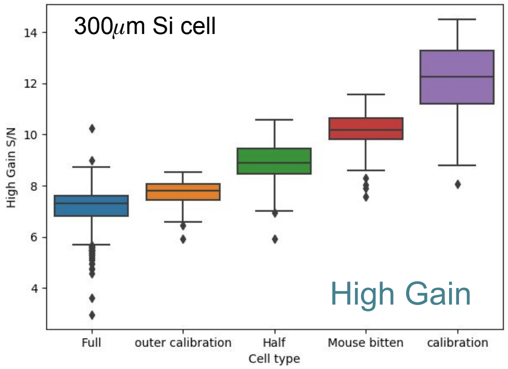

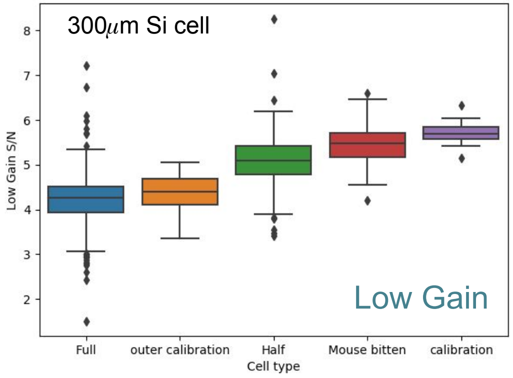

S/N dependence on cell type shows smaller cell area → higher S/N.

This result helps us to decide noise rejection threshold for further data analysis as we shall see in the further slides.

ADC response to the charge injection

- The response of the different ADC gain stages was also measured using charge injection data.
- In the charge injection method, the channels are injected with a known charge in a controlled environment in laboratory, and the ADC responses of different ADC gain stages are measured.
- The plot on right shows ADC responses of **high-gain** , **low-gain** and **ToT** as a function of input charges expressed in terms of MIP units.
- High-gain stage is sensitive to smaller signals and is used for energy deposited upto ~ 50 MIPs.
- Low-gain stage used for energy deposited from ~ 50 to 250 MIPs.
- ToT is used for energy deposited beyond 250 MIPs.

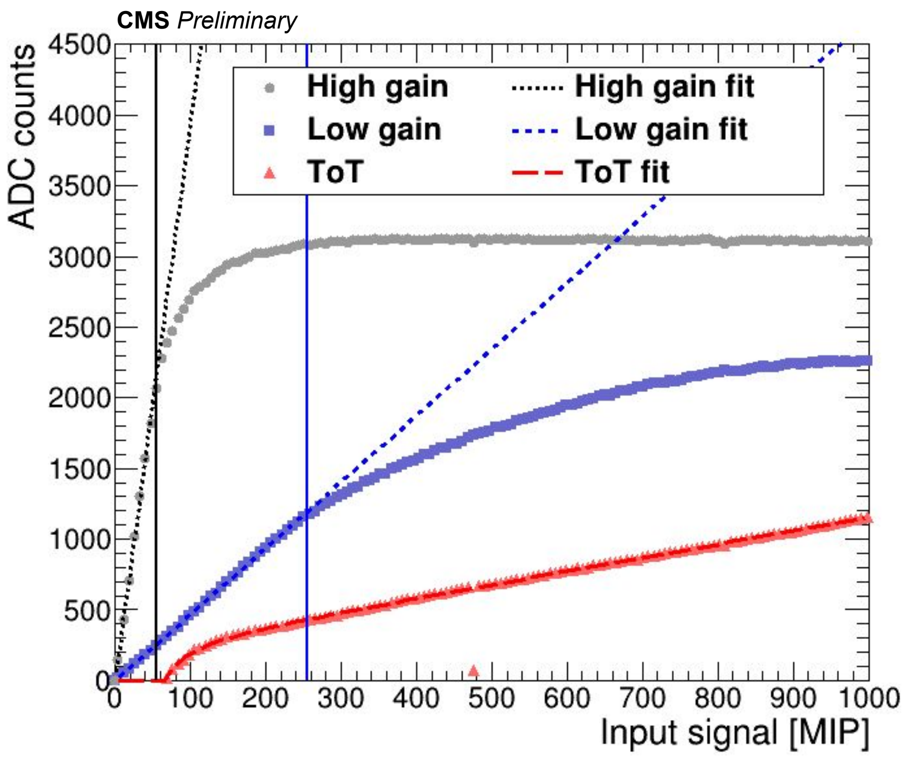

Tracking in parasitic runs

- Muon beam used during October 2018 TB, was not wide enough to cover all the silicon cells.
  - Channel-to-channel calibration could not be performed for all cells using muon beam.
- After the standard test beam run, the setup was left operating and was exposed to muons (among others) of unknown energy which were remnants particles coming from upstream experiment.
- To select the cells with traversing muons, the calorimeter was used as a tracking device.
- Hits in consecutive layers were fitted with a straight line and were selected to obtain MIP energy distribution.

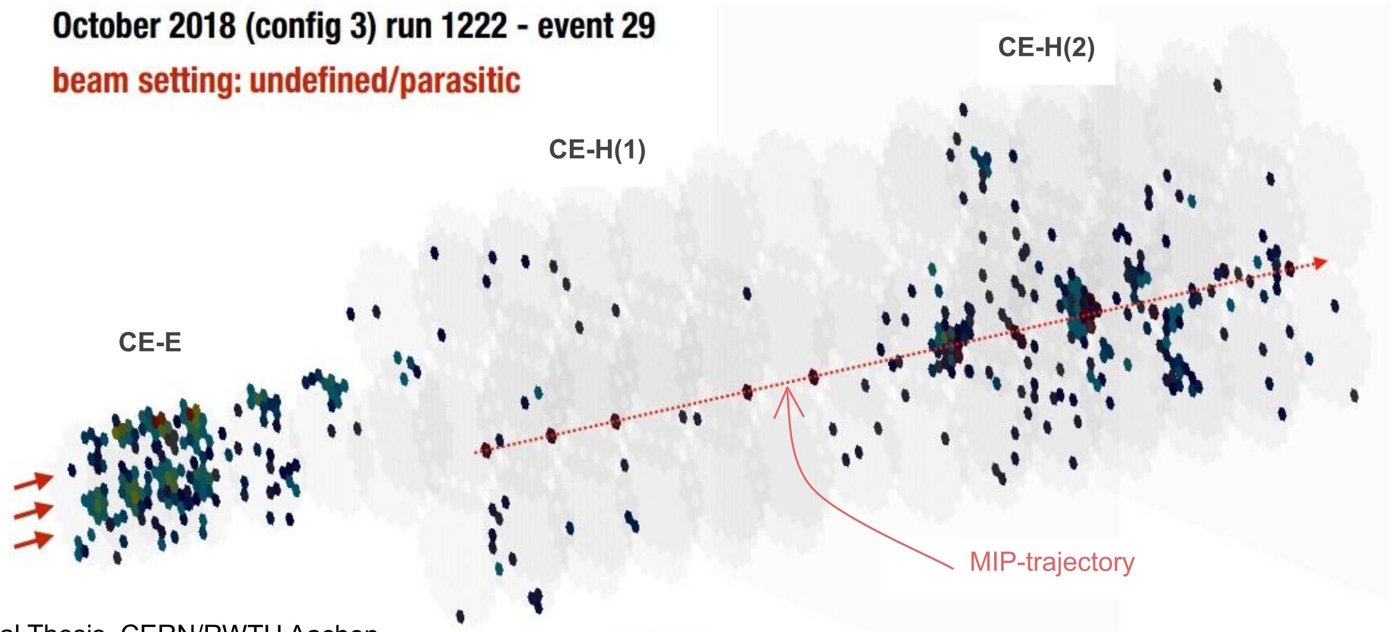

Reference: Thorben Quast, Doctoral Thesis, CERN/RWTH Aachen

Simulation and physics lists

- Beam test experimental setup geometry and particle interaction with the detector material is simulated using Geant4[1] package integrated in CMS software's framework (CMSSW).

- Geant4 provides different processes[2] to model EM and hadronic interactions with the detector.

- EM Model:
  - EMN : For all EM interactions such as ionization, Bremsstrahlung, pair production etc.
- Hadronic Model:
  - BERT : Bertini intra-nuclear cascade model intended for incident energy between 100 MeV and 9 GeV
  - FTFP : Based on the FRITIOF description of string excitation and fragmentation, intended for incident energy above 4 GeV
  - QGSP : Quark gluon string model, intended for incident energy above 12 GeV.

- Different models are combined together to make a physics-list. Often the ranges of validity overlap between these models.

- Beam test experiment data is used to validate the simulation framework and physics models.

References:
[1] S. Agostinelli et al., GEANT4 — a simulation toolkit, Nucl. Instrum. Meth. A 506 (2003) 250.
[2] Geant4, guide for physics lists

Data-MC comparison at MIP level

- The starting point for pion analysis is the **energy reconstructed in terms of number of MIPs** using ***muons*** both in data and simulation.
    - More details about gain linearization & channel-to-channel calibration in data can be found in construction & commissioning paper: 2021 JINST 16 T04002.
- In CE-E & CE-H simulation, detailed electronics noise has not been simulated. Therefore, the MIP signal is smeared by a width of $1/6^{th}$ of a MIP to account for electronics noise.
- AHCAL - reconstructed data (in terms of number of MIPs) & full simulation framework are provided by the CALICE collaboration.

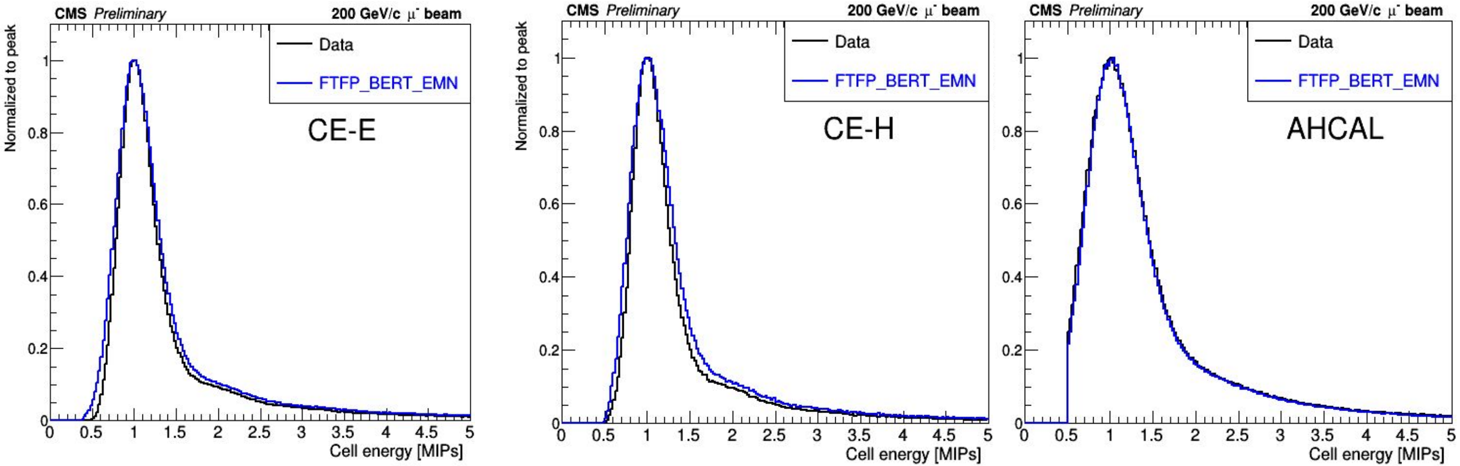

Muon signal is reasonably well produced by simulation in all compartments

- The MIP signal peaks at 1 in both data and MC muon samples.
- There are minor differences in width in CE-E & CE-H which could be improved with realistic digitization.

Data cleaning

- A set of cleaning cuts are applied to remove undesired events such as beam contamination, out-of-acceptance particle incidence etc.

Applied per channel

- **Channel masking:** Mask channel with H/W issues.
- **Noise rejection:** 3σ and 4σ noise rejection HG ADCs CE-E and CE-H prototype, respectively.

Applied per event

- **Track quality cut:** At least 3 hits out of 4 DWCs & χ^2/ndf of reco track < 10
- **Muon veto:** To reject muon contamination.
- **Track-window cut:** Reject events where incident particle out-of-acceptance i.e. it is way off-center.
- **Pre-showering pion rejection:** Rejects early showering pions (layer <=2).

- The effect of each cleaning cut is shown in following two plots for total energy sum (CE-E+CE-H+AHCAL) in data..

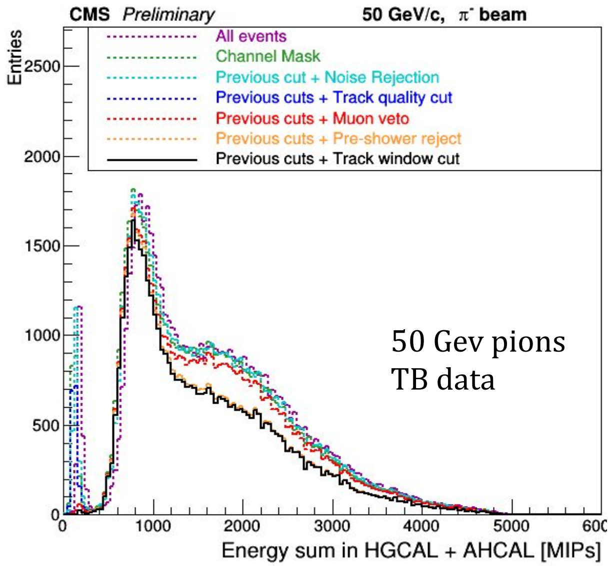

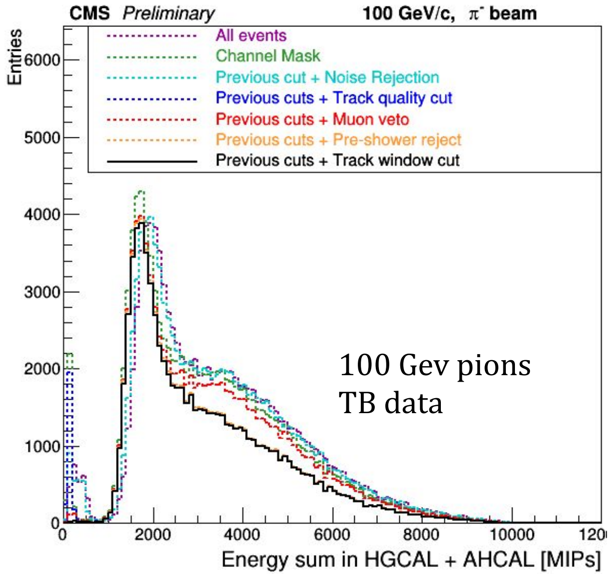

The cleaning cuts are applied on both data and simulation for consistency.

Depth of first hadronic interaction

(Shower start finder algorithm)

High granularity of CE-E and CE-H prototype allows us to develop an algorithm to identify the location of first hadronic interaction of pion where it initiates showering.

Example event display
October 2018 TB: **Run 515 - event 12**
300 GeV pion

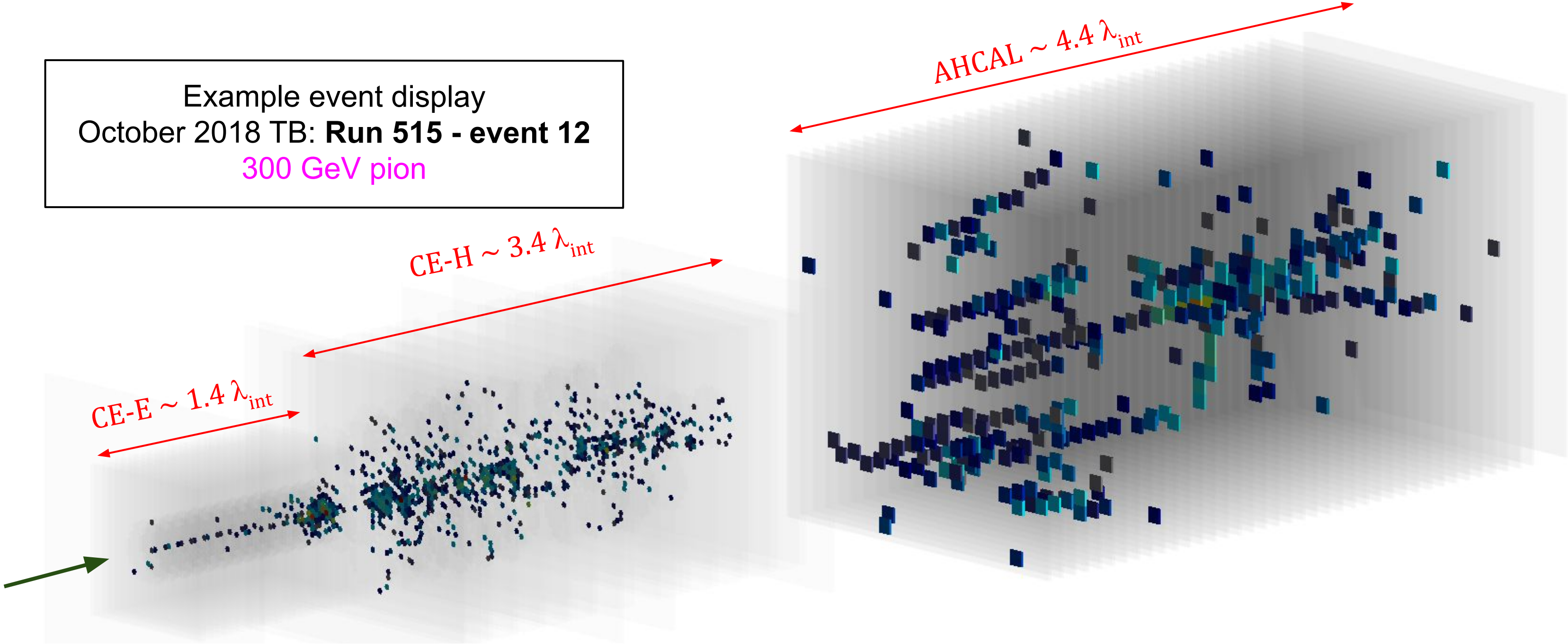

Shower start finder algorithm
(Optimization and validation)

- Hadrons develop a shower in the detector when interact with the nucleus of detector material via strong interaction.

- Number of surviving hadrons without starting a shower, falls exponentially as it penetrates deeper into the detector.
  - Denser the material, higher will be the probability of starting a shower.

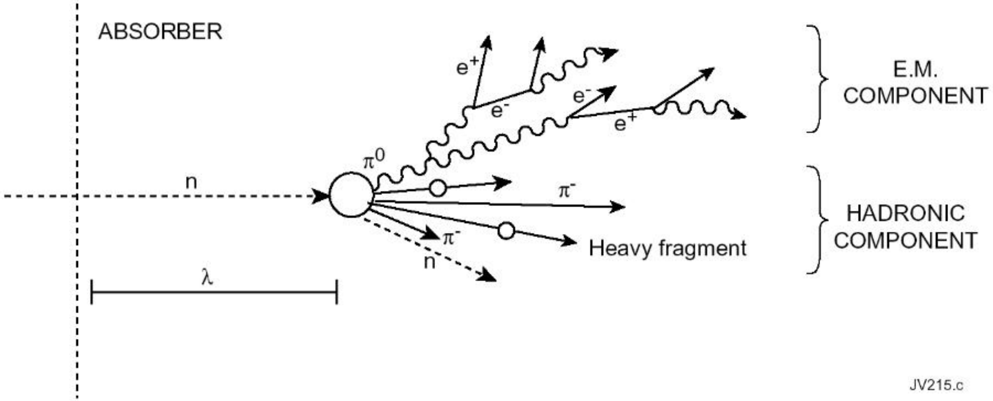

$$N = N_0 \times exp(\frac{-x}{\lambda_{int}})$$

Exponential decay relation

- With the help of truth information from the simulation and reconstructed observatables from experimental data, we develop an algorithm that identifies the location of first hadronic/nuclear interaction.

- The algorithm is optimized and then validated against truth value to maximize the performance.

Extraction of true first hadronic interaction

- Events are simulated using CMSSW's **Geant4** package.
  - Geant4 is simulation framework that provides detector geometry building environment as well as physics models to simulation particle's interaction with detector material.

- In Geant4, each particle is tracked and propagated in steps, called *G4Step.*

- Based on a physics model and particle type, there are various interactions that a G4Step can undergo (e.g. ionization, bremsstrahlung etc).

- If the primary particle (i.e. particle shot from the particle gun) undergoes hadronic interaction then following information is saved:
  - (x,y,z) position of first hadronic interaction of primary track..
  - Number of secondaries produced at the interaction point.
  - particleIDs, charge, (x,y,z) coordinates of each secondary particle.
  - Kinetic energies carried by the each secondary particle.

- To get the shower start location in the HGCAL TB setup, z-coordinate is projected onto the next active layer.
  - Because shower start finder algorithm will give the shower start location in terms of layer number.

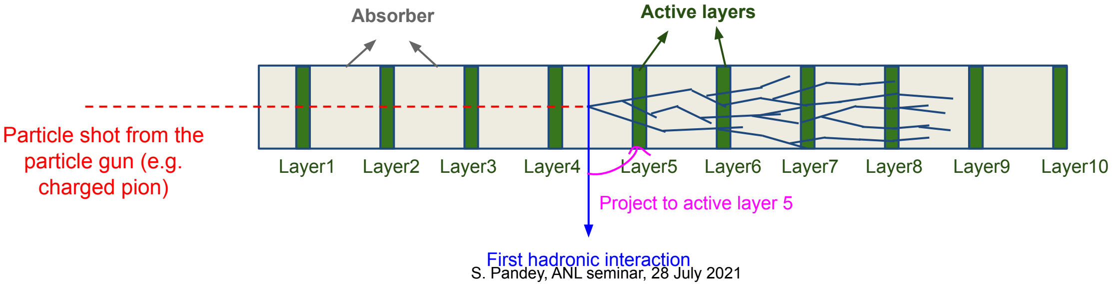

Selection of “hard” hadronic interaction

- In simulation, hadronic interaction includes both soft and hard hadronic interaction.

- For example, if we look at the event display of one of the 20 GeV pion event, we find that “truth” information indicates that the first hadronic interaction occurred at layer = 12.

- But shower does not start until later layers of CE-H.

- These “soft” interaction needs to be removed in order to optimize shower start finder algorithm.

- In these soft hadronic interactions, we expect that number of secondaries will be small and momentum transfer to secondaries will be minimum.

- We need to tag these events and remove it from optimization sample.

- In the next slide, I will discuss how events are tagged.

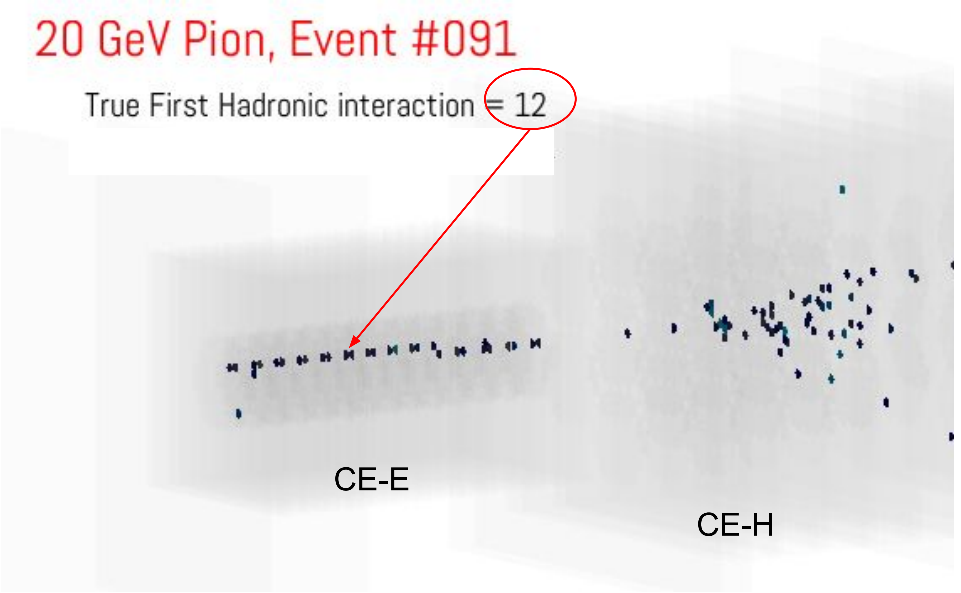

Selection of "hard" hadronic interaction (Contd..)

- We look at the correlation plot of "number of secondary particles" vs "Fractional kinetic energy carried by the secondaries".

- Since in Geant4, it is not possible to distinguish between incident hadron after the hadronic interaction therefore "kinetic energy carried by secondaries" is estimated as follows:
  - Among all the secondary particles, the KE of leading hadron of same species (π- in this case) is subtracted from the sum of KE of all the secondaries. Then it is normalized by the beam energy in order to facilitate a single cut across all beam energies.

- Following two plots show correlation plot of "number of secondary particles" vs "Fractional kinetic energy carried by secondaries" for 20 GeV (left) and 100 GeV (right plot).

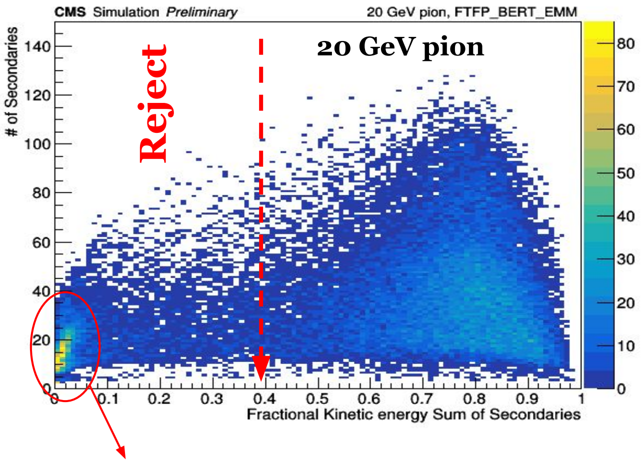

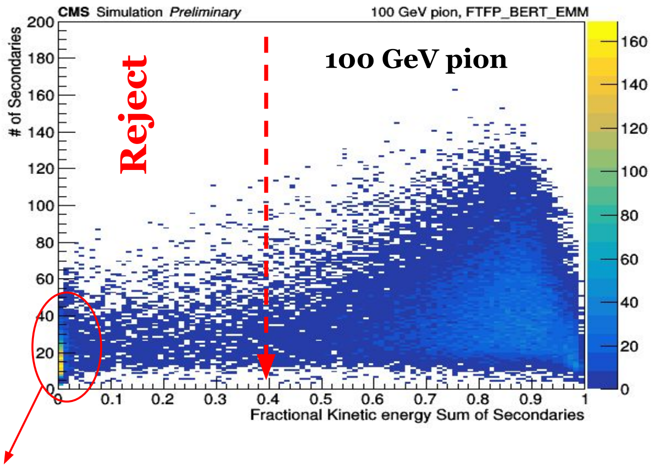

Events for which Fractional KE sum of secondaries are less than 0.4 are rejected.
Rejection rate:
20 GeV = 18.7%
100 GeV = 14%

Small number of secondary produced in the hadronic interaction and low momentum transfer

Algorithm optimization

- To identify the shower start location, we optimize the algorithm using number of hits, energy deposition and lateral shower spread.
- We use muons as a reference for differentiating against showering pions to optimize the thresholds on these observables.

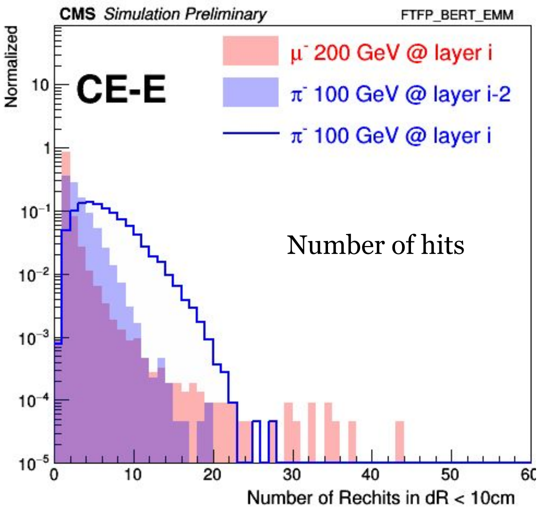

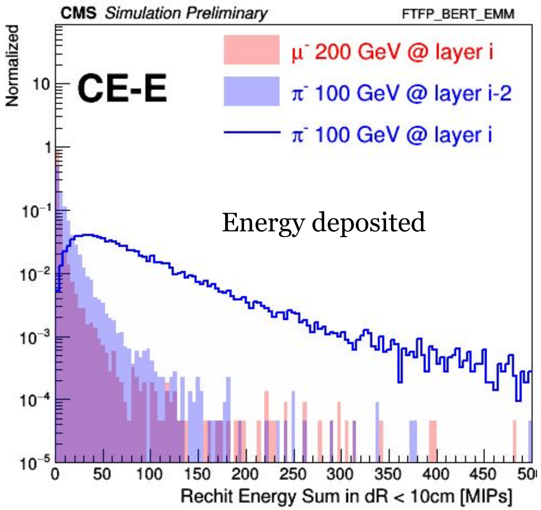

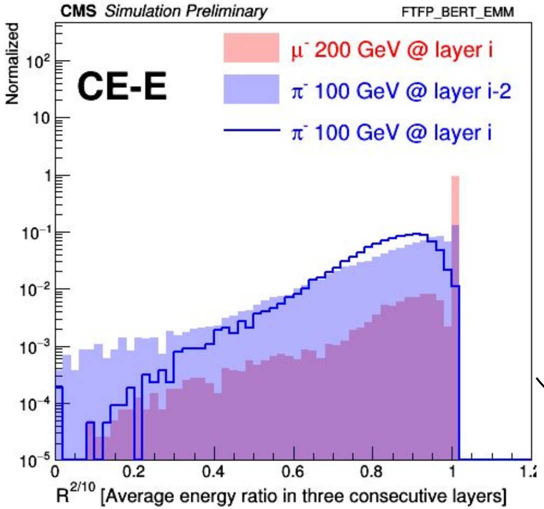

Algorithm

1. Compute Nrechit^{10cm}_i, En^{10cm}_i and $R^{2/10}\_avg\_i$ at layer i
2. If ($\text{Nrechit}^{10cm}\_i > 3$ && $\text{En}^{10cm}\_i > E\_thres$ && $R^{2/10}\_avg\_i < 0.96$) ⇒ Shower started at layer i and Exit
3. If (i == End_of_HGCAL_layers) ⇒ Shower start not found and Exit, Else ⇒ Go to Next layer and repeat.

Lateral energy ratio

$$R\_avg^{i}_{(2/10)} = \frac{\sum_{j=i}^{i+2} En^{j}_{2cm}}{\sum_{j=i}^{i+2} En^{j}_{10cm}}$$

Efficiency of shower start finder algorithm

- The performance of the algorithm is assessed in terms of **efficiency** defined as **the fraction of events for which the predicted layer falls within ±n layers of GEANT4-true shower start layer.**
- Efficiency is compared for different GEANT4 physics lists.

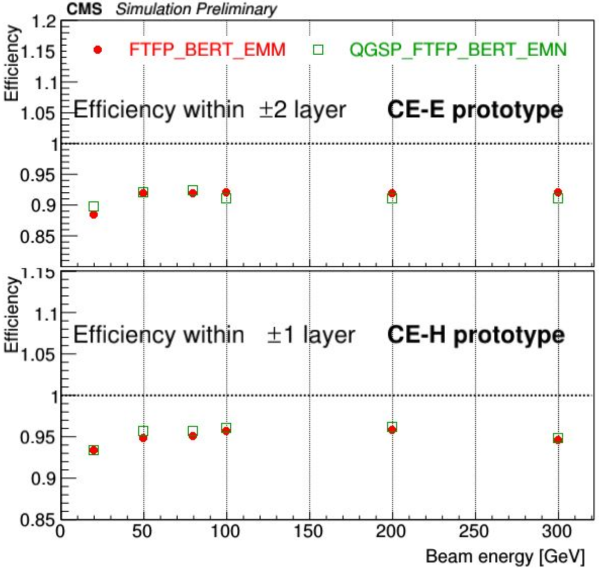

- The algorithm shows consistent efficiency across all beam energies:
  - The efficiency is ≧ 90% & 95% for ±2 layers for CE-E and for ±1 layer CE-H prototype, respectively.

- When employed in beam test data it shows exponentially falling behaviour, as expected.
- Very well agreement with simulation.

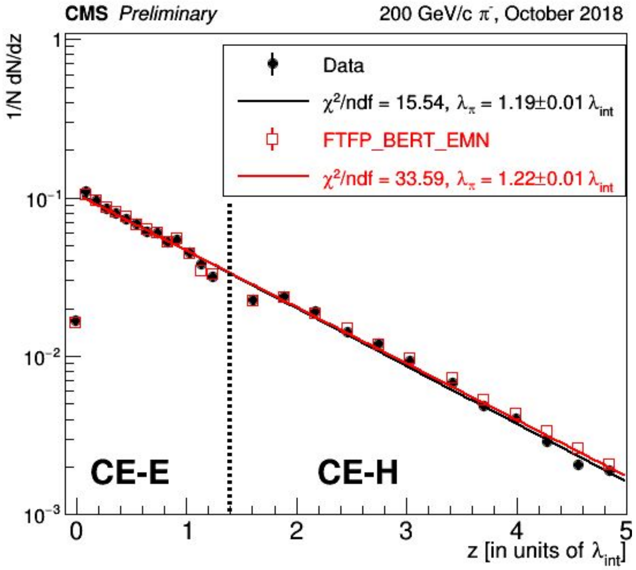

Event categorization:

`If (Shower-start-layer <= 28)` := Showering in CE-E

`Else If (Shower-start-layer > 28)` := MIPs in CE-E

`Else`: Reject events

MIP-to-GeV conversion factors

Pion shower energy reconstruction:

Showering in CE-E:

$E^{measured}$ [in GeV] $= \alpha^{fix} * E^{CE-E}_{[MIPs]} + \beta^{fix} * (E^{CE-H}_{[MIPs]} + \gamma^{fix} * E^{AHCAL}_{[MIPs]})$

MIPs in CE-E:

$E^{measured}$ [in GeV] $= \beta^{fix} * (E^{CE-H}_{[MIPs]} + \gamma^{fix} * E^{AHCAL}_{[MIPs]})$

For CE-E:
α^{fix} = **10.6 MeV/MIP** using 50 GeV e^+

For CE-H + AHCAL:
β^{fix}= **78.9 MeV/MIP** using 50 GeV π^-

γ^{fix} = *relative_weight* between CE-H & AHCAL = **0.4**

To find energy scale CE-H+AHCAL, we use 50 GeV pions which are MIPs in CE-E.

- Since the sampling fraction of CE-H and AHCAL are different therefore it is important to introduce a relative weight factor.
  - Relative weight between CE-H & AHCAL (γ^{fix}) is obtained by minimizing resolution (scan over different values of weight).
- After fixing this γ^{fix}, find overall MIP-to-GeV (β^{fix}) for CE-H+AHCAL.

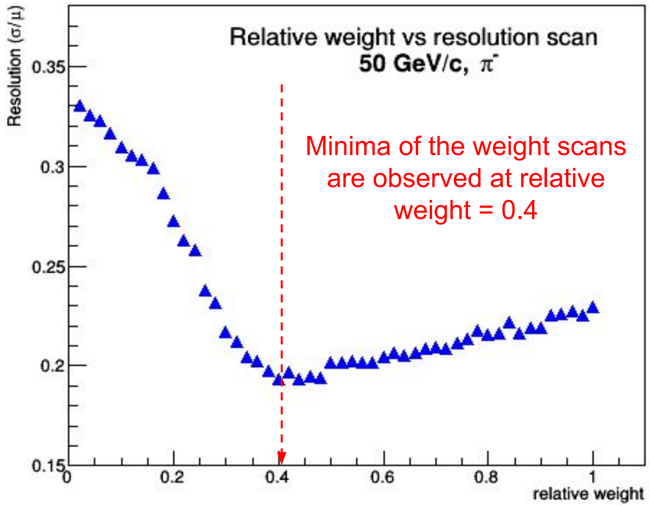

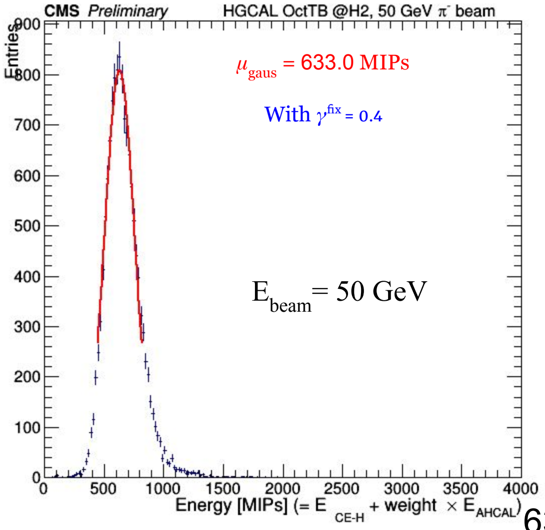

Distributions comparison in data & MC

- **Using the same α^{fix} , β^{fix}, γ^{fix} obtained from the data**, we compare energies measured in simulation with that in data.
- Plots show comparison between data and simulation for 100 GeV pions that start showering and that are MIPs in CE-E.

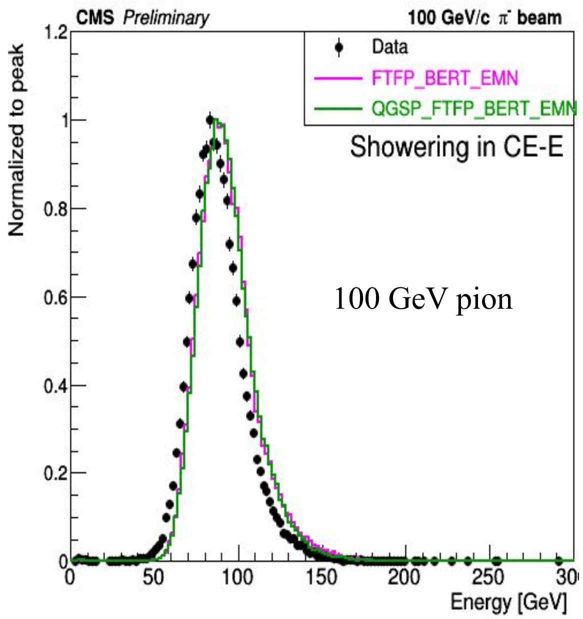

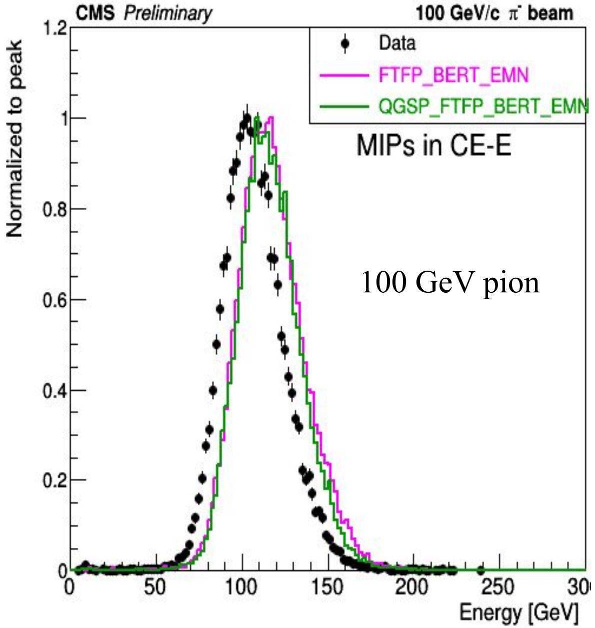

- The energy distribution shape is reproduced well by simulation.
- However, simulation distribution is shifted towards higher response.
  - We check this for other energies in terms of response by fitting a Gaussian function around the core of the energy distribution.

χ^2 optimization of weights

- The energy response can be linearized by obtaining energy-dependent weights using chi2-minimization.

- For pions showering in CE-E (EH pions):
  - E^{corr} [in GeV] = $\alpha_1(E_{beam}) * E^{CE-E}_{fix} + \beta_1(E_{beam}) * E^{CE-H}_{fix} + \gamma_1(E_{beam}) * E^{AH}_{fix}$

- For pions MIPs in CE-E (H pions):
  - E^{corr} [in GeV] = $\beta_2(E_{beam}) * E^{CE-H}_{fix} + \gamma_2(E_{beam}) * E^{AH}_{fix}$ + 0.4 GeV

- Construct and minimize $\chi 2$ analytically to obtain the weights.
  - CE-E/CE-H/AHCAL energy is already set to GeV with fixed weights.
  - σ(E) is the uncertainty in the measured energy obtained with fixed-weights.
  - 0.4 GeV offset corresponds to MIP track energy deposit in CE-E.

$$\chi^2 = \sum_{pions} \frac{(E_{beam} - E^{EH}_{corr})^2}{\sigma^2(E)}$$

$$\frac{\sigma^{EH}(E)}{E} = \frac{139\%}{\sqrt{E}} + 8.4$$

$$\frac{\sigma^{H}(E)}{E} = \frac{125\%}{\sqrt{E}} + 8.9$$

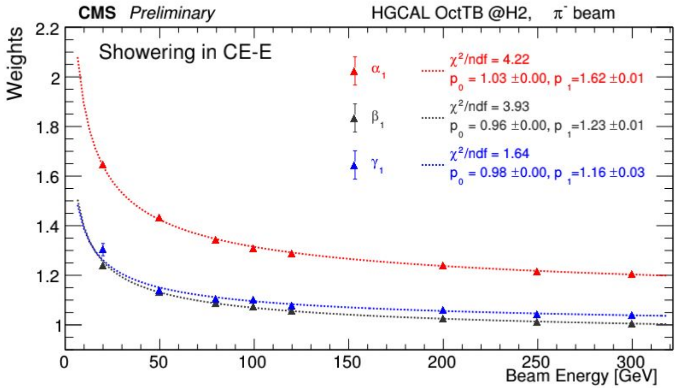

- **The weights are determined using TB data** and are applied on both data and simulation.

- In the real experiment, track momenta is taken as a reference to extract energy-dependent weights.
  - For neutral hadrons or beyond tracker coverage, calorimeter energy measured using fixed weights (method-1) is taken as a reference.
  - We fit the weights with a polynomial function, and evaluate the weights from the fitted function.

Response and resolution data-MC comparison

- Response and resolution is compared between data and simulation with both physics lists after applying optimized weights as shown below. (**Energy rescaling is applied on MC to match data.**)

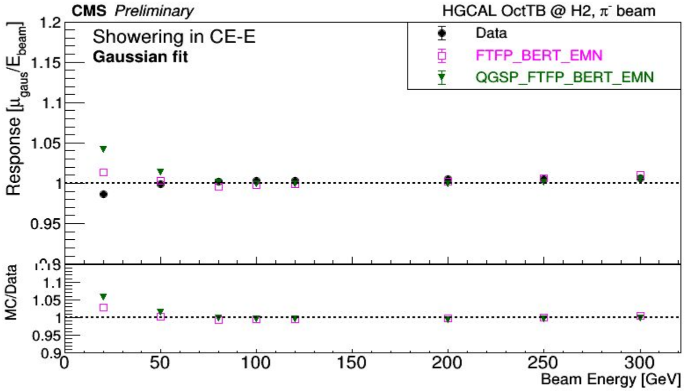

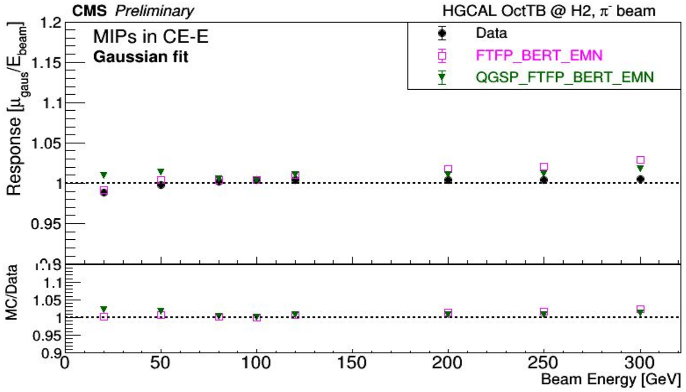

Response: Agreement within ~5% between data and MC.

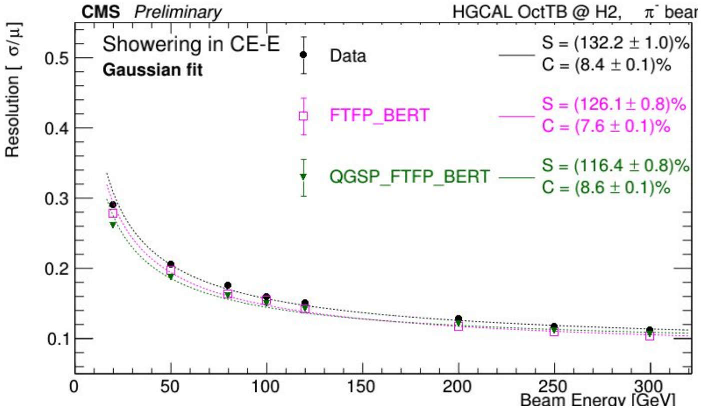

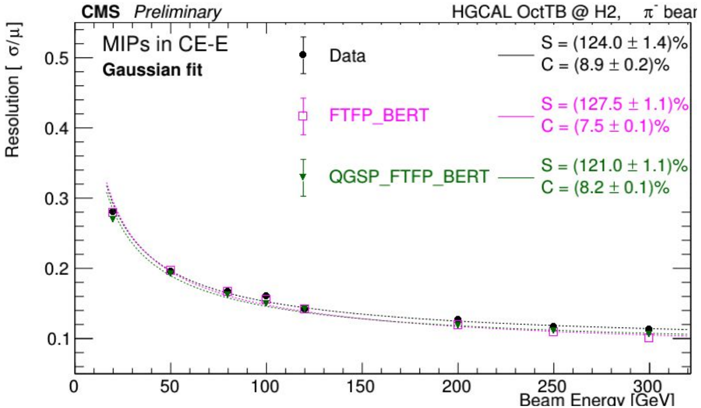

Resolution

- **Showering in CE-E:** Better agreement at higher energies & slight difference at lower energies. Overall agreement 1- 10% at low energies .

- **MIPs in CE-E:** Better agreement at higher energies & slight difference at lower energies. Overall agreement within 10%.

Beam test setup: Detector prototype

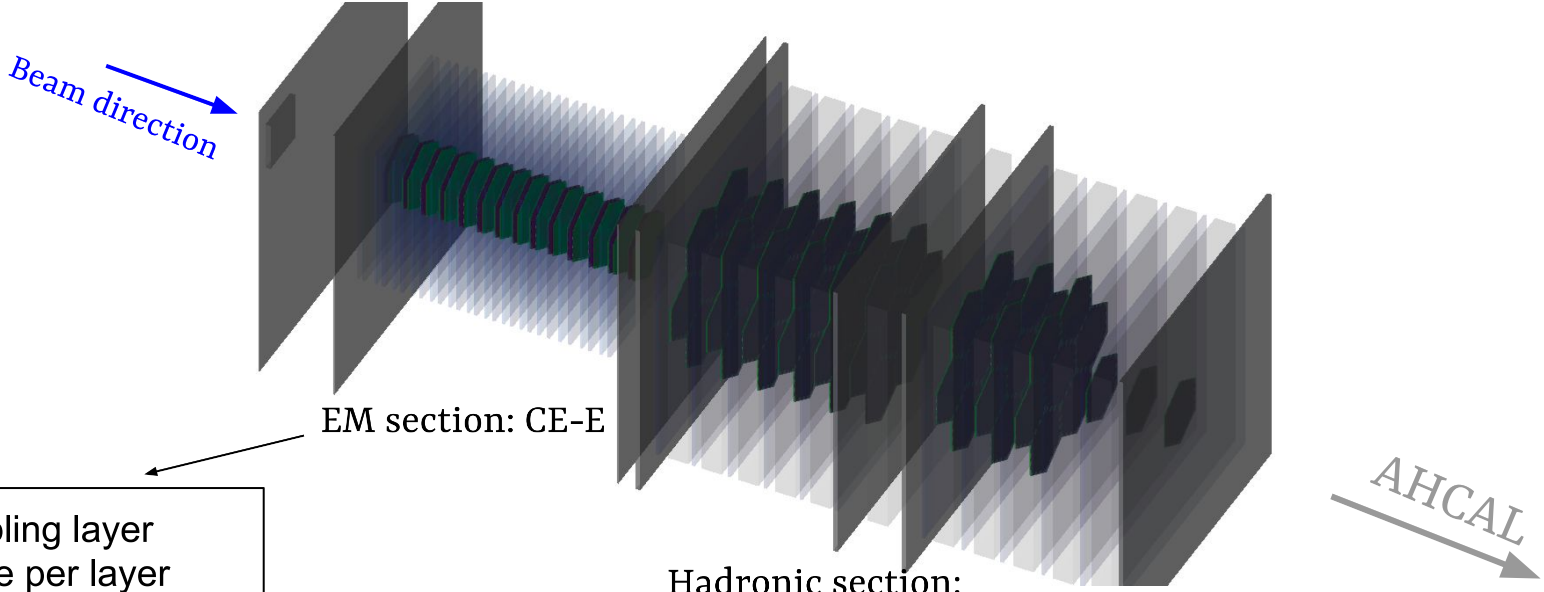

- 28 sampling layer
- 1 module per layer
- **Pb/Cu/CuW absorber**
- **~ 26 X_0, 1.4 λ_{int}**

- 12 sampling layer
- 7 modules per layer in first 9 layers
- 1 module per layer in last 3 layers
- **Steel absorber**
- **~ 3.4 λ_{int}**

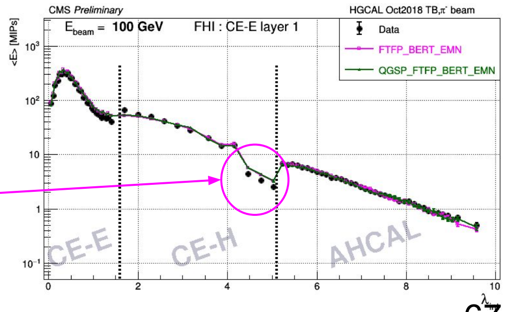

Detector setup: Useful informations

- We have higher sampling in EM section as compared to Had section.
  - **28 sampling in 1.4 λ_{int} in CE-E** vs **12 sampling in 3.4 λ_{int} in CE-H.**
- We have different absorbers in EM section and Had section.
  - **Pb/Cu/CuW in CE-E** and **steel (Fe) in CE-H.**

Iron (Fe) is proxy for steel here.
Couldn't find the actual values for steel alloy on pdg

Lead (Pb)
- Atomic number : 82
- Atomic mass : 207
- Density : 11.35 g cm^{-3}
- Radiation length (X_0) : 0.5612 cm
- Pion interaction length (λ_{pion}): 19.93 cm

Iron (Fe)
- Atomic number : 28
- Atomic mass : 55.8
- Density : 7.87 g cm^{-3}
- Radiation length (X_0) : 1.757 cm
- Pion interaction length (λ_{pion}): 20.42 cm

- Observation:
  - $\mathbf{X_0}$ of Pb is about 3x smaller than Fe
  - $\boldsymbol{\lambda_{pion}}$ of Pb and Fe is almost similar.
- Given the small $\mathbf{X_0}$ in Pb as compared to $\boldsymbol{\lambda_{pion}}$, the EM component of shower will be almost fully contained in a few layers of CE-E while hadronic component of shower continue to evolve into the CE-H.

Nature of hadronic showers

- It has two components:
  - EM component: from π^0 → instantly decays to two γ
  - Hadronic component

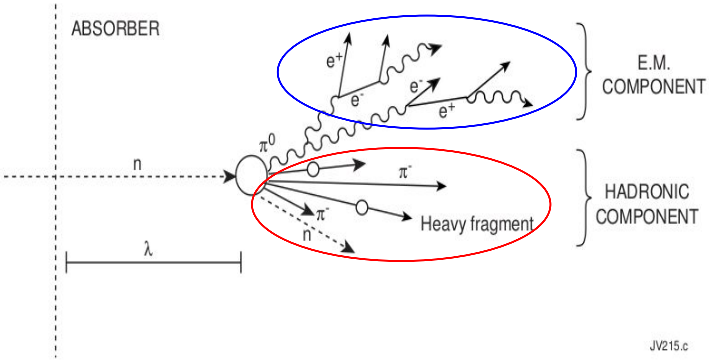

- For same incident energy of pion and electron:
  - EM shower has more secondary particles as compared to hadronic shower.
  - In our setup, we have:
    - 100 GeV e^+ → approx. 10000 MIPs in CE-E
    - 100 GeV π^- → approx. 1500 MIPs in CE-H

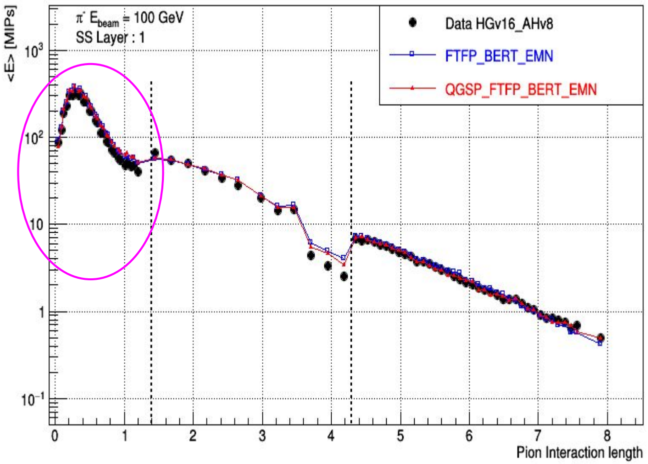

- Taking above two points into consideration along with the fact that ~28 X_0 of Pb is enough to contain almost all of EM shower.
  - Are we probing into EM component of pion shower in CE-E compartment?
  - To check this, we make use truth information of secondary particles, generated at first hadronic interaction (similar to shower start finder algorithm optimization).

Number of neutral pions at first hadronic interaction

- Using the same handle, we plot the distribution of fractional energies carried by π^0's produced at the first interaction.
  - No cut is applied on π^0 energies.
  - Neutral pions produced at the first interaction has been considered in this study.
  - Neutral pions are produced at later interactions also, especially for higher incident energies.

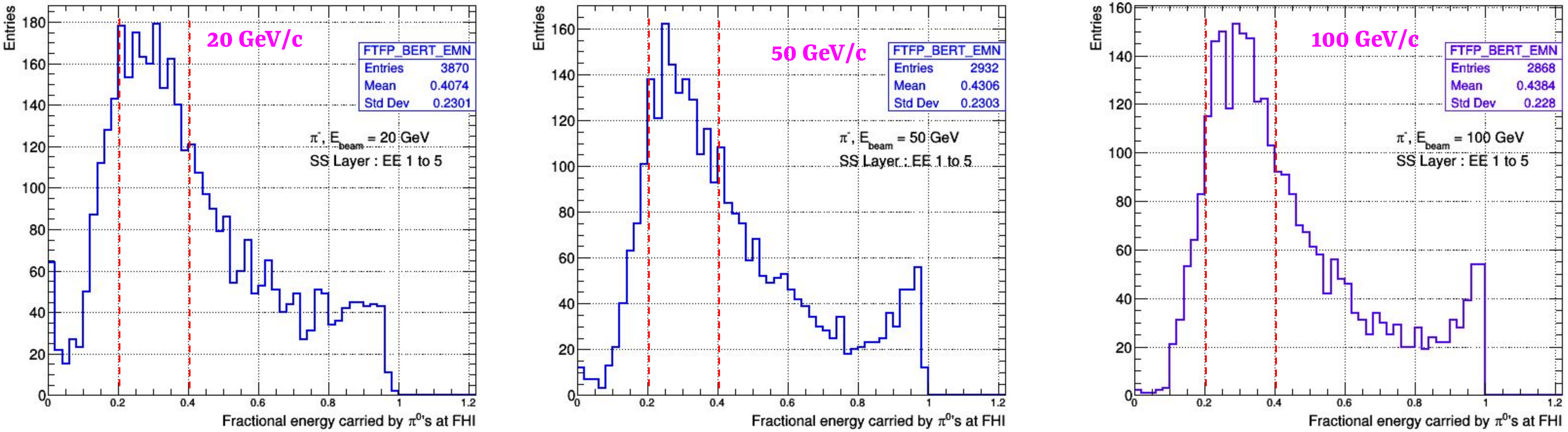

Plot the shower shapes again, but now divide them into separate categories. (See next slide)

Shower shapes in different categories

- Following two plots show, longitudinal shower shapes for 50 GeV/c pion (left) and 100 GeV/c pions (right) in three different categories based on fraction energies carried by pi0's at the first hadronic interaction.
  - Inclusive in shower starting in first five layers.

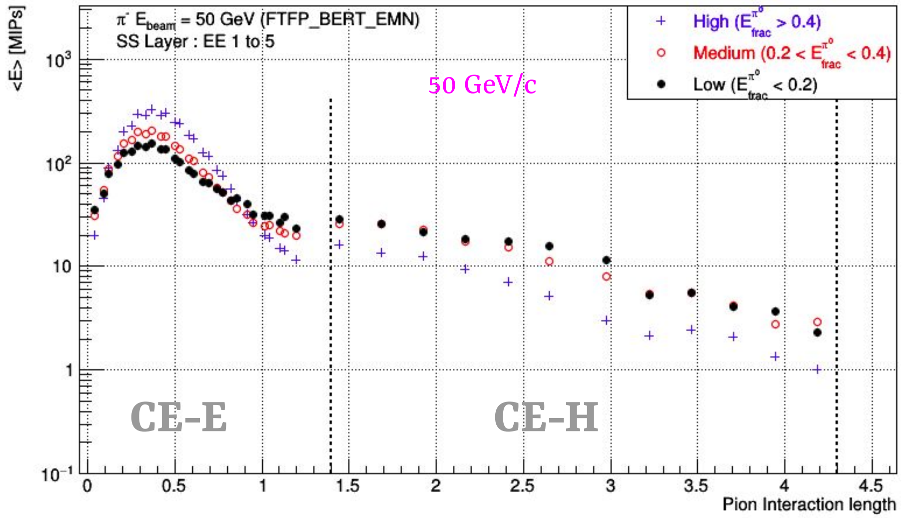

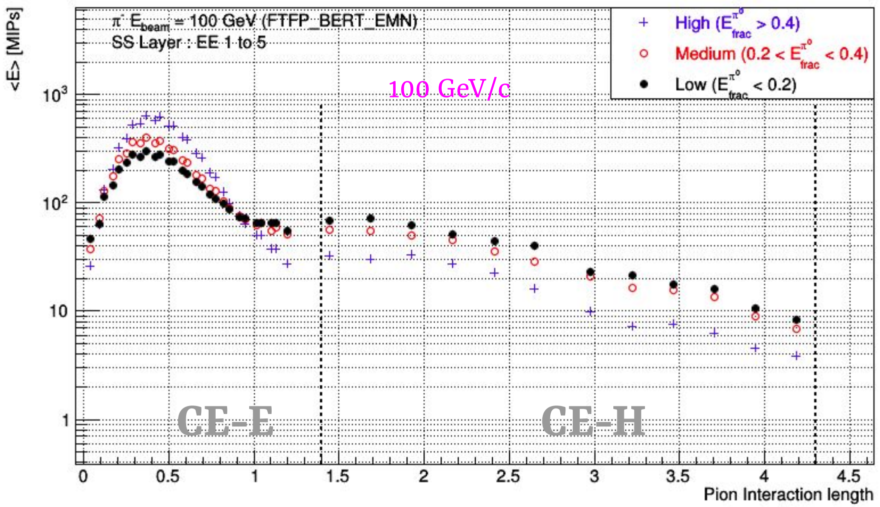

- Average energy deposited:
  - **Higher in CE-E and lower in CE-H when E_{frac} > 0.4 → higher EM fraction → mostly contained in CE-E**
  - **Lower in CE-E and higher in CE-H E_{frac} < 0.2 → higher had fraction → mostly contained in CE-H**

Shift of shower maximum

- Following plots show average energy deposited [MIPs] as a function of **"layer"** for three shower starting points for 100 GeV/c π^{-} beam.

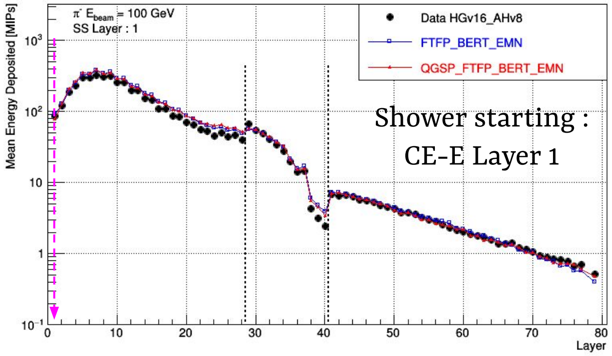

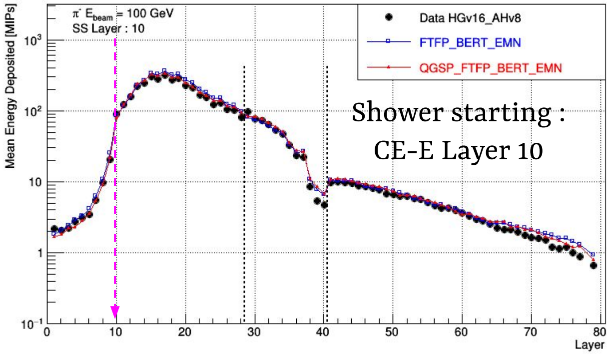

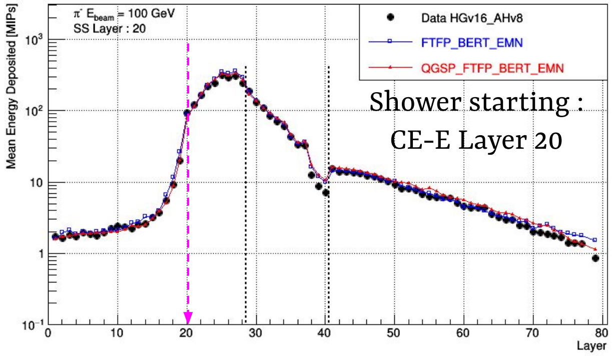

- Shower maximum lies ~ 7 layers away from shower starting point.
- Shower maxima for 30-50 GeV positron lies at around 8-9.
- These studies indicates that the first peak that we see in the shower shapes is dominated by EM component of hadronic shower.
- We are able to probe the π^{0} component with our fine longitudinal sampling of CE-E prototype !!

Variable used to study transverse shower shapes

- Variable: energy weighted distance from the center of gravity at ith layer.
  - Accentuates lateral spread according to energy deposited.

Center of Gravity at layer - i

$$x^i_{CG} = \frac{\sum_j x^i_j \times E^i_j}{\sum_j E^i_j} \;;\; i \in [1,40] \text{ and } j \in [\text{rechits at layer i}]$$

$$y^i_{CG} = \frac{\sum_j y^i_j \times E^i_j}{\sum_j E^i_j} \;;\; i \in [1,40] \text{ and } j \in [\text{rechits at layer i}]$$

Energy weighted distance from CG of rechit - j

$$dR^{\text{weighted}}_j = \sqrt{(x_j - x_{CG})^2 + (y_j - y_{CG})^2} \times E_j$$

Larger lateral spread
Moderate lateral spread
Least lateral spread

Highest energy at the center and dies down as we move radially outward.

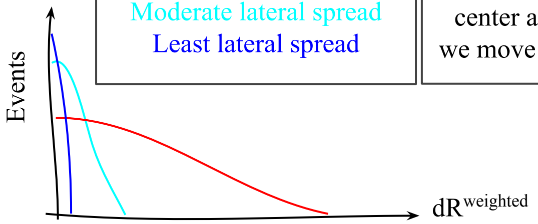

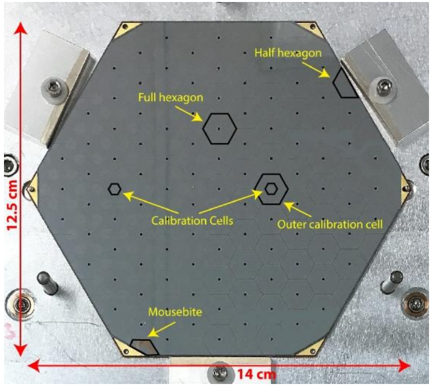

CE-E prototype layer

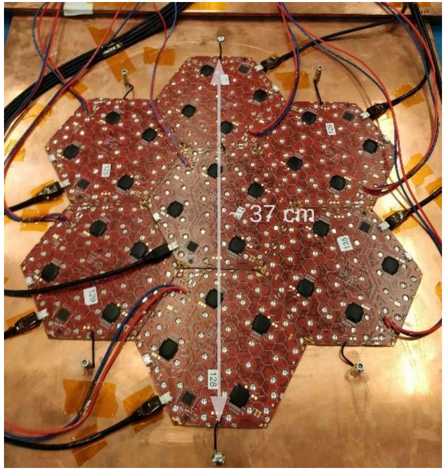

CE-H prototype layer

Point to remember:
CE-H prototype layer has considerably larger area than CE-E layer.

Transverse shower shapes at different depths (Contd…)

Shower start location: CE-E layer 1-7

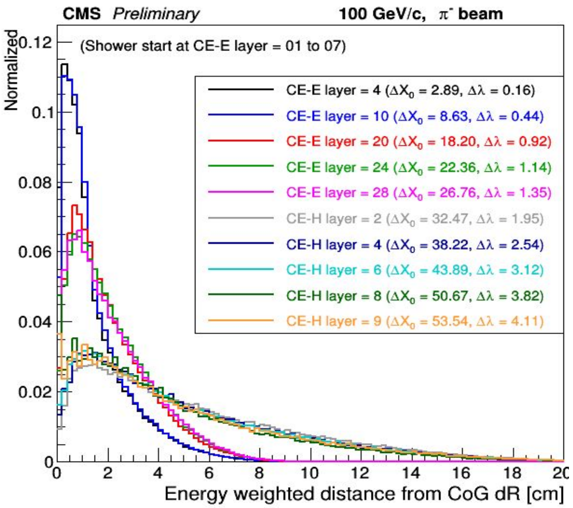

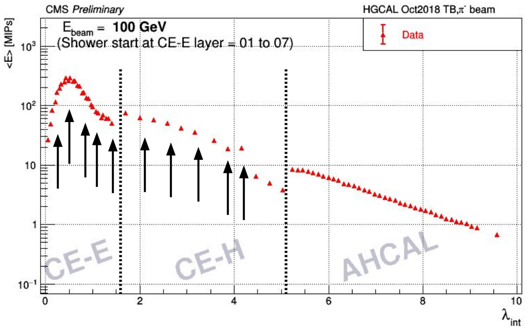

Shower start location: CE-H layer 1

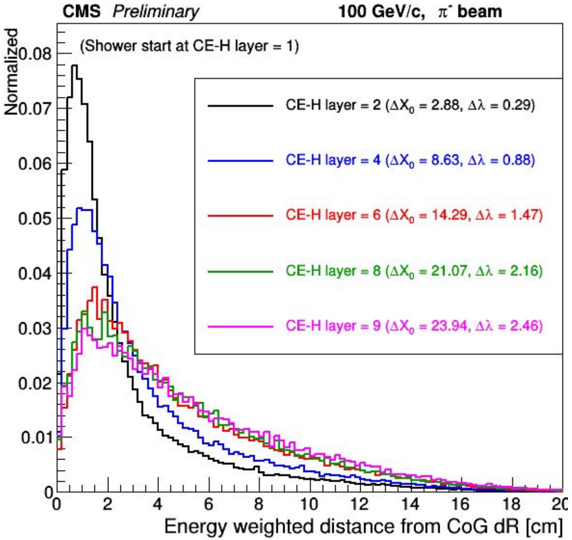

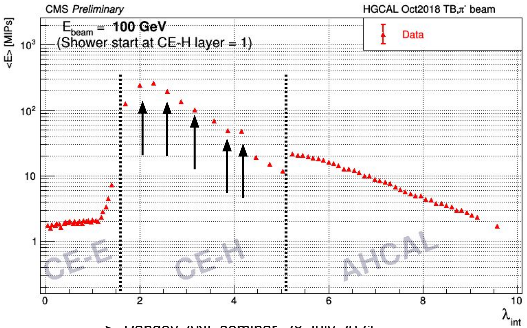

For shower starting in CE-H also, we observe narrower spread around the the peak.

Though the spread is larger as compared to SS in CE-E.

Possible reasons:

- More modules in CE-H.
- For similar **ΔX_0** in CE-H, **Δλ** is ~2x as compared to CE-E → more space for hadronic component to spread in CE-H.